UNIVERSITA' VITA-SALUTE SAN RAFFAELE

CORSO DI DOTTORATO DI RICERCA INTERNAZIONALE IN MEDICINA MOLECOLARE

Curriculum in Medicina Clinica e Sperimentale

INTERFERING WITH MEVALONATE PATHWAY TO UNLEASH EFFECTIVE ANTITUMOR RESPONSE IN MELANOMA

Supervisore: Prof. Vincenzo Russo

Co-supervisore: Prof. Gianpietro Dotti

Tesi di DOTTORATO di RICERCA di Giuseppe Damiano

Matr. 022112

Ciclo di dottorato XXXVIII

SSD MED/06

Anno Accademico 2024/2025

UNIVERSITA' VITA-SALUTE SAN RAFFAELE

CORSO DI DOTTORATO DI RICERCA INTERNAZIONALE IN MEDICINA MOLECOLARE

Curriculum in Medicina Clinica e Sperimentale

INTERFERING WITH MEVALONATE PATHWAY TO UNLEASH EFFECTIVE ANTITUMOR RESPONSE IN MELANOMA

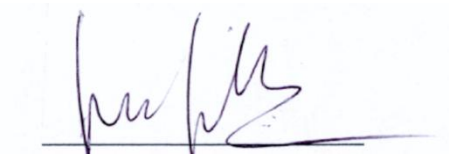

Supervisore: Prof. Vincenzo Russo

Co-supervisore: Prof. Gianpietro Dotti

Tesi di DOTTORATO di RICERCA di Giuseppe Damiano

Matr. 022112

Ciclo di dottorato XXXVIII

SSD MED/06

Anno Accademico 2024/2025

CONSULTAZIONE TESI DI DOTTORATO DI RICERCA

Il sottoscritto Giuseppe Damiano

Matricola 022112

nato a Varese (VA)

il 11/07/1989

autore della Tesi di Dottorato di Ricerca dal titolo:

Interfering with mevalonate pathway to unleash effective antitumor response in melanoma

☒ AUTORIZZA la Consultazione della Tesi

□ NON AUTORIZZA la Consultazione della Tesi per …… mesi a partire dalla data di sottomissione della domanda di conseguimento titolo

Poiché:

□ l'intera ricerca o parti di essa sono potenzialmente soggette a brevettabilità;

□ ci sono parti di Tesi che sono già state sottoposte a un editore o sono in attesa di pubblicazione;

□ la Tesi è finanziata da enti esterni che vantano dei diritti su di esse e sulla loro pubblicazione

Data ……26/01/2026…… *Firma* 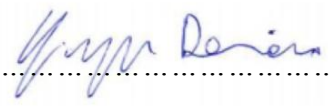

DECLARATION

This thesis has been:

- composed by myself and has not been used in any previous application for a degree. Throughout the text I use both 'I' and 'We' interchangeably.
- has been written according to the editing guidelines approved by the University.

Permission to use images and other material covered by copyright has been sought and obtained.

All the results presented here were obtained by myself, except for:

1) *Peripheral blood mononuclear cells (PBMCs) and the clinical database of patients with metastatic melanoma were made obtained through a collaboration with the Melanoma Department directed by Dr. Paolo A. Ascierto, Cancer Immunotherapy and Development Therapeutics, Istituto Nazionale Tumori IRCCS Fondazione G. Pascale, Naples, Italy.*

2) *The Statistical analysis of the clinical database of patients with metastatic melanoma (results presented in Chapter 4, Figure 6 and Table 3) was conducted in collaboration with Dr. Giovanni Paolino, Unit of Dermatology, IRCCS San Raffaele Scientific Institute, Milan, Italy.*

3) *The analysis of the high-dimensional flow cytometry data (results presented in Chapter 4, Figures 8, 9, 12, and 13) was performed in collaboration with Dr. Achille Anselmo, Advanced Cytometry Technical Applications Laboratory (FRACTAL), IRCCS Scientific Institute San Raffaele, Milan, Italy.*

All sources of information are acknowledged by means of reference.

Abstract

Immune checkpoint inhibitors (ICIs) have significantly improved survival in metastatic melanoma; however, most patients eventually experience disease progression and death. Emerging evidence suggests that statin therapy, widely prescribed for cardiovascular comorbidities, may potentiate ICIs efficacy, although the underlying mechanisms remain incompletely understood.

Taking advantage of a unique clinical records of 66 patients with metastatic melanoma, including 20 receiving statin therapy concomitantly with anti-PD1, we found that statin use was associated with improved progression-free survival (PFS) and overall survival (OS). Intriguingly, the improved clinical outcome correlated with the increased frequency of activated circulating monocytes prior to ICI administration. These clinical observations were corroborated by in vivo studies. In B16-bearing mice, simvastatin pre-treatment enhanced the antitumor activity of anti-PD1 and was accompanied by increased activation of intratumor dendritic cells (DCs). To investigate the mechanism, we first assessed the direct effects of statin on DCs founding that simvastatin markedly enhanced DC maturation and functional activation. We next explored how this effect occurs demonstrating, through targeted inhibition experiments, that simvastatin-induced DC activation was mediated by isoprenoid depletion and p38 MAPK activity.

Overall, our findings support a model in which statins, by promoting the activation of antigen presenting cells, can contribute to establish a tumor microenvironment more responsive to immune checkpoint blockade. Further studies are needed to better define the precise molecular pathways involved. Nonetheless, given their favorable safety profile and widespread clinical use, our results provide strong rationale for prospective trials evaluating statin-ICI combination strategies in malignancies where ICIs are standard-of-care.

Abstract

Gli inibitori dei checkpoint immunitari (ICIs) hanno significativamente migliorato la sopravvivenza nel melanoma metastatico; tuttavia, la maggior parte dei pazienti sperimenta ancora progressione di malattia e morte. Evidenze emergenti suggeriscono che la terapia con statine, ampiamente prescritta per le comorbidità cardiovascolari, possa potenziare l'efficacia degli ICIs, sebbene i meccanismi alla base di questo fenomeno non siano ancora completamente chiari.

In una coorte di 66 pazienti con melanoma metastatico, di cui 20 in trattamento concomitante con statina e anti-PD1, abbiamo osservato che l'uso di statine si associa ad un miglioramento della progression-free survival (PFS) e della overall survival (OS), oltre che a una maggiore frequenza di monociti circolanti attivati prima della somministrazione degli ICIs. Queste osservazioni cliniche sono state ulteriormente confermate in vivo: nei topi portatori di melanoma B16, la simvastatina ha aumentato l'attività antitumorale dell'anti-PD1 ed è risultata accompagnata da una maggiore attivazione delle cellule dendritiche (DCs) intratumorali. Per approfondire il meccanismo alla base di questo effetto, abbiamo innanzitutto valutato l'impatto diretto della statina sulle DCs, riscontrando che la simvastatina promuove in modo marcato la loro maturazione e attivazione funzionale. Abbiamo successivamente indagato come tale effetto venga mediato, dimostrando, tramite esperimenti di inibizione selettiva, che l'attivazione delle DCs indotta dalla simvastatina è dipendente dalla deplezione degli isoprenoidi e dall'attività di p38 MAPK.

Complessivamente, i nostri risultati supportano un modello secondo cui le statine, favorendo l'attivazione delle cellule presentanti l'antigene, contribuiscono a creare un microambiente tumorale più responsivo al blocco dei checkpoint immunitari. Saranno tuttavia necessari ulteriori studi per definire con precisione le vie molecolari coinvolte. Nonostante ciò, dato il loro favorevole profilo di sicurezza e l'ampio utilizzo clinico, i nostri dati offrono un razionale solido per studi prospettici volti ad indagare strategie di combinazione tra statine e ICIs nei tumori solidi in cui gli ICIs rappresentano lo standard terapeutico.

TABLE OF CONTENTS

Chapter 1

INTRODUCTION

1.1 Cutaneous melanoma: overview

Cutaneous melanoma is a malignant neoplasm originating from melanocytes, which are the cells responsible for melanin production. Embryologically, melanocytes arise from neural crest and are primarily located in the epidermis. Its prevalence is steadily increasing worldwide, largely due to uncontrolled exposure to sunlight and to the use of artificial tanning devices[1]. Approximately 85% of melanoma diagnoses occur in patients from North America, Europe, and Oceania. The current incidence in individuals aged over 25 years is estimated at 20-30 new cases per 100,000 inhabitants in North America and Europe, and up to 60 cases per 100,000 inhabitants in Australia and New Zealand[2]. In Italy, melanoma is the second most common cancer under the age of 50 in males and the third in females, with around 12.700 new diagnoses estimated in 2022[3].

Like most malignant tumors, melanoma arises from a progressive accumulation of genetic mutations that confer characteristics such as uncontrolled proliferation, resistance to apoptosis, and immune evasion. In Caucasian populations, most melanomas are attributed to the mutagenic effects of ultraviolet radiation (UVR), even if UVR alone is not enough. Melanoma results from a complex interplay between UVR-induced oncogenic mutations such as those affecting BRAF, NRAS and KIT, inherited genetic predispositions including CDKN2A and BAP1 mutations, and phenotypic factors such as skin phototype, sun sensitivity, and the number and type of cutaneous nevi[4–6].

Diagnosis of melanoma is histological, although clinical suspicion can initially arise through naked-eye examination using the ABCDE criteria (asymmetry, border irregularity, color variation, diameter > 6 mm, and evolution over time). However, confirmation is typically achieved through dermoscopy which, when performed by a trained and experienced dermatologist, allows for the identification of suspicious lesions even when small in size. Paradoxically, these small lesions are often the most critical to detect, as early-stage melanoma can be cured through surgical excision alone, without the need for further investigations or therapies. This underscores the importance of prevention, particularly through routine dermatological evaluations in individuals with fair skin phototypes.

Melanoma prognosis is closely linked to initial staging, with two main factors determining it: Breslow thickness and the presence or absence of metastasis in regional lymph nodes. These two parameters form the basis of the widely used AJCC staging

system and guide the referral of all patients with a Breslow thickness ≥ 0.8 mm, in the absence of distant metastases, for sentinel lymph node biopsy[7].

Fortunately, most melanomas are diagnosed at stage I, with only about 5% of cases identified at stage IV. As illustrated in Figure 1 and 2, stage I patients have a 10-years melanoma-specific survival rate > 90%. For stage II, 10-years survival ranges from 88% (IIA) to 75% (IIC), while stage III 10-years survival is more heterogeneous ranging from 88% in stage IIIA to 60% in stage IIIC. Stage IIID melanoma is a more rare entity with a poorer prognosis comparable to that of metastatic disease.[8]

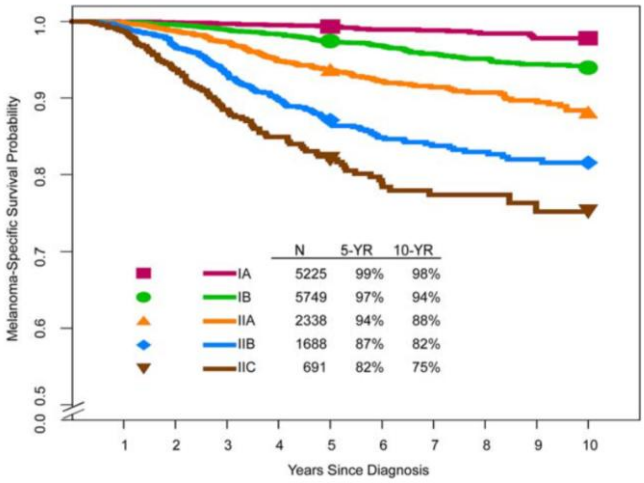

Figure 1. Kaplan-Meier curves of melanoma-specific survival for Stage I and II disease, based on the AJCC Eighth Edition International Melanoma Database.

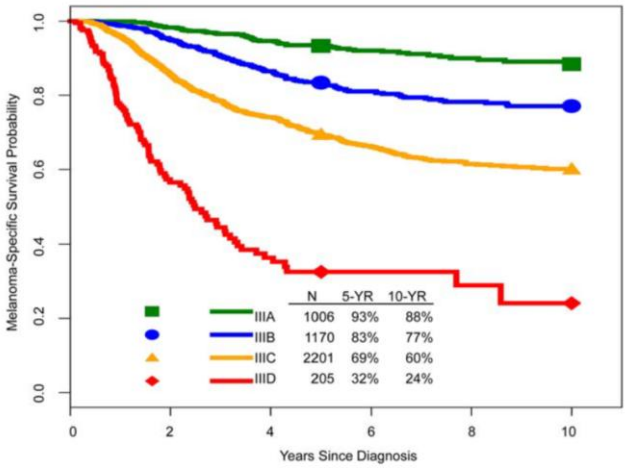

Figure 2. Kaplan-Meier curves of melanoma-specific survival for Stage III subgroups, based on the AJCC Eighth Edition International Melanoma Database.

As regards stage IV, 5-year overall survival (OS) has recently reached 52%, largely due to the advent of combination immunotherapy with Nivolumab and Ipilimumab, marking a turning point in the treatment of this chemo-refractory malignancy[9]. However, it should be acknowledged that OS outcomes reported in pivotal clinical trials may overestimate survival compared with unselected real-world populations, owing to patient selection, controlled treatment delivery, and optimized follow-up. Real-world studies have nonetheless confirmed a substantial improvement in survival in the immunotherapy era, albeit with generally lower absolute OS rates than those observed in clinical trials[10,11]. Notably, survival has also significantly improved in stage III and, more recently, stage IIB–IIC melanoma following the introduction of adjuvant therapies[12–14], and their impact is expected to become increasingly evident in population-based survival estimates in future AJCC staging updates.

As we propose with this work to demonstrate how metabolic pathways, particularly the mevalonate pathway, can enhance the efficacy of immunotherapy, the following sections will focus on immunotherapy. However, it is important from a therapeutic perspective to highlight that approximately 50% of melanomas harbor the BRAFV600 somatic mutation, which acts as a key driver of the disease[15]. This mutation tends to be more frequent in less sun-exposed areas, such as the trunk, and in patients with a high nevus count and intermittent sun exposure. These patients, in addition to immunotherapy, can benefit from targeted therapy, both in the adjuvant and metastatic settings. Even targeted therapy, when administered as first-line therapy for metastatic disease, has had a significant impact, increasing the 5-year OS of these patients to 34-35%, as demonstrated in phase III clinical trials[16,17].

1.2 Immune checkpoint inhibition in metastatic melanoma

Since 2010, when the first clinical data on the anti-CTLA-4 antibody ipilimumab were published[18], checkpoint inhibitor therapy has radically transformed the prognosis of metastatic melanoma, leading from a median survival of less than 12 months with chemotherapy to a 5-year OS of approximately 50%[9]. The CheckMate-067 phase III randomized trial remains the most impactful study in terms of survival benefit. Recently published 10-year data confirmed the long-term efficacy of nivolumab plus ipilimumab, with a 10-year OS of 43%, compared to 37% with nivolumab alone and 19% with

ipilimumab alone. 10-year progression-free survival (PFS) showed a similar trend, reaching a plateau after 3 years (Figure 3). Median-OS was 71.9 months for the combination, 36.9 months for nivolumab, and 19.9 months for ipilimumab[19]. Similarly, the Keynote-006 trial compared pembrolizumab to ipilimumab in 834 patients. The 5-year OS was 38.7% for pembrolizumab versus 31% for ipilimumab, and 4-year PFS was 23% versus 7.3%. No significant differences were observed between the two dosing schedules of pembrolizumab (every 2 vs 3 weeks)[20]. Lastly, the RELATIVITY-047 trial introduced relatlimab, the first anti-LAG-3 monoclonal antibody to be approved for cancer treatment, in combination with nivolumab. At 3-years, OS was 54.6% for the combination versus 48% for nivolumab alone, and 3-years PFS was 31.8% versus 26.9%[21] (Figure 4). The combination showed a favorable safety profile when compared with nivolumab-ipilimumab and is increasingly used in patients where CTLA-4 toxicity is a concern.

These data supported nivolumab-ipilimumab combination as the first-line treatment of choice for eligible patients. Nivolumab-relatlimab is preferred in patients at risk of CTLA-4-related toxicity, offering better efficacy than monotherapy but less than the nivolumab-ipilimumab combo. Monotherapy with nivolumab or pembrolizumab remains a valid option, especially in frail patients or those with low disease burden. Ipilimumab alone is now reserved for second-line use after progression on anti-PD-1 therapy[7].

Patients affected by BRAFV600-mutant melanomas may also benefit from targeted therapy. The DREAMseq and the SECOMBIT trials have clarified that starting with immunotherapy yields better long-term outcomes than initiating with BRAF/MEK inhibitors[22,23]. Interestingly, BRAF-mutant patients in these studies performed even better than wild-type counterparts. However, a subset (~20%) of patients may experience a rapid progression of the disease with immunotherapy (Figure 5 and 6) and currently, no biomarkers can reliably predict this risk. Consensus suggests that patients with symptomatic disease and/or poor performance status may benefit more from targeted therapy first, due to its rapid antitumor activity and high objective response rate (~70%).

Stage IV patients with brain metastases require special consideration. In asymptomatic patients not requiring more than 10 mg/day of prednisone equivalent corticosteroids, combination immunotherapy is the preferred first-line approach, regardless of BRAF status. This is supported by data from CA209-204, ABC trial, and NIBIT-M2, which

showed improved efficacy of combinatorial immunotherapy only in asymptomatic patients[24–26]. For symptomatic patients, instead, targeted therapy is preferred if BRAF-mutated; otherwise, single-agent immunotherapy may be considered, though prognosis remains poor. A multidisciplinary approach involving neurosurgeons and radiation oncologists is essential for the management of brain metastases, to evaluate surgical or locoregional options alongside systemic therapy.

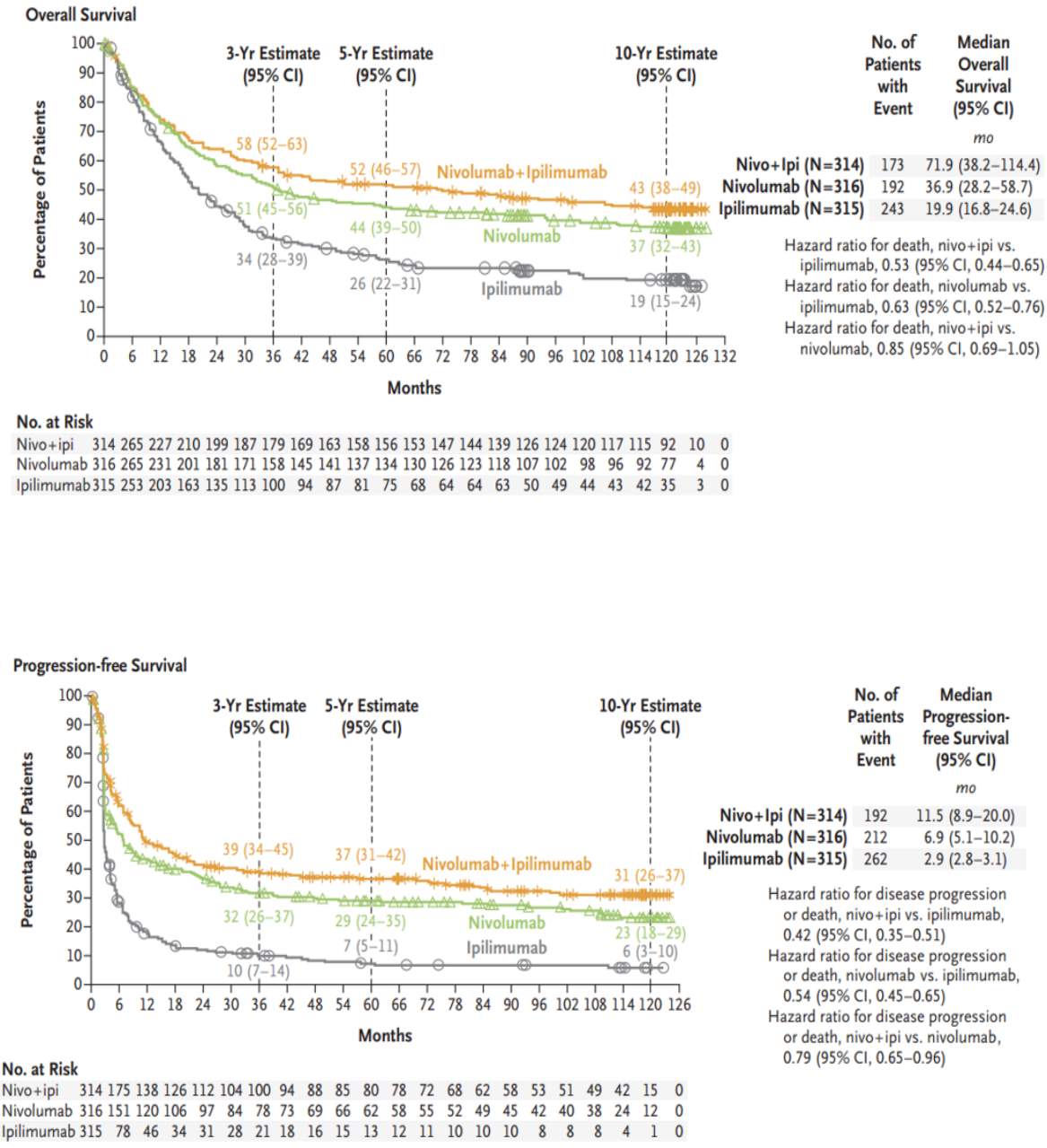

Figure 3. OS and PFS in patients treated with nivolumab plus ipilimumab, nivolumab alone, or ipilimumab alone. Data reproduced from the Checkmate 067 trial[19].

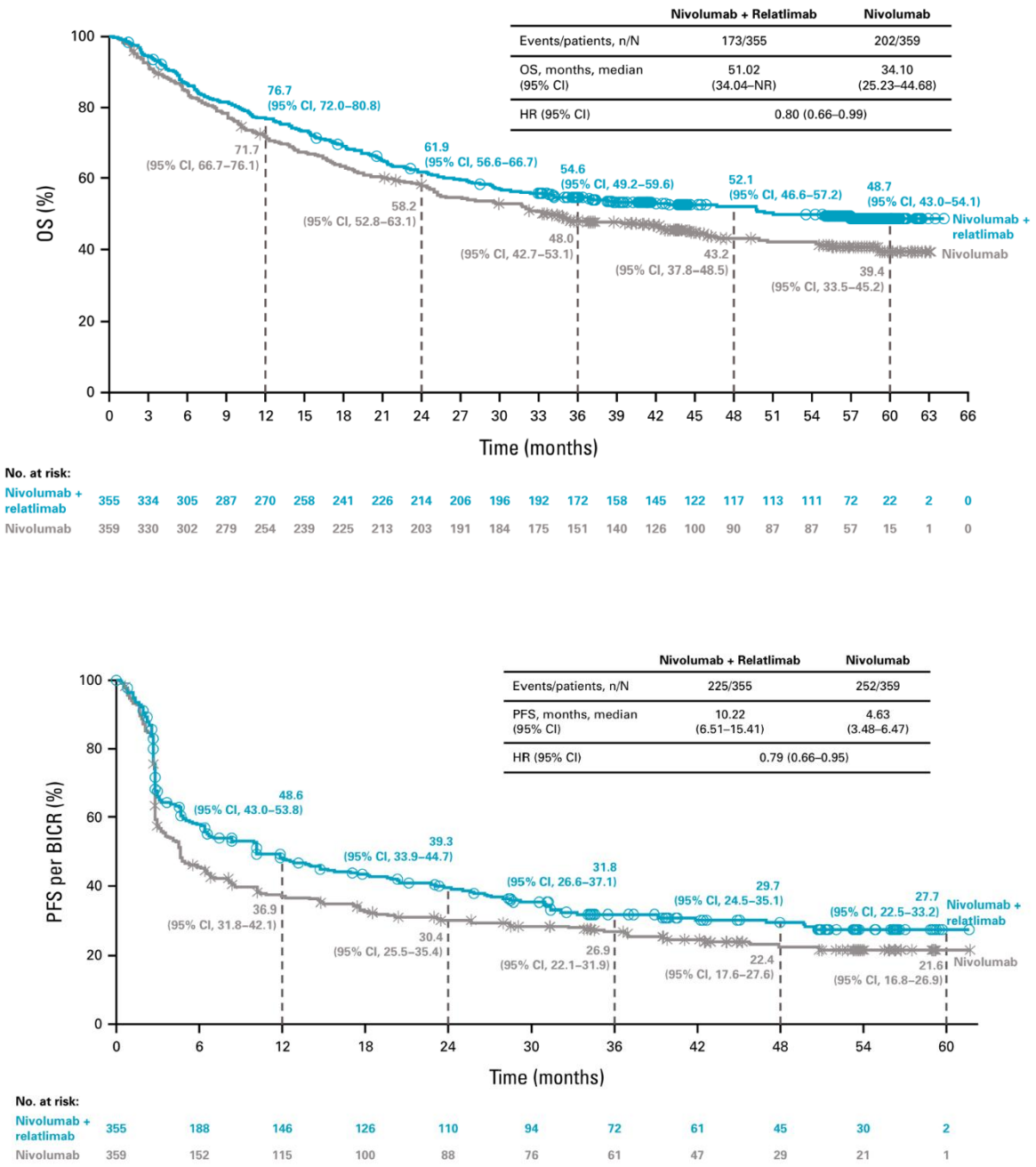

Figure 4. OS and PFS in patients treated with nivolumab plus relatlimab or nivolumab alone. Data reproduced from the Relativity-047 study[21].
BICR, blinded independent central review; HR, hazard ratio; NR, not reached.

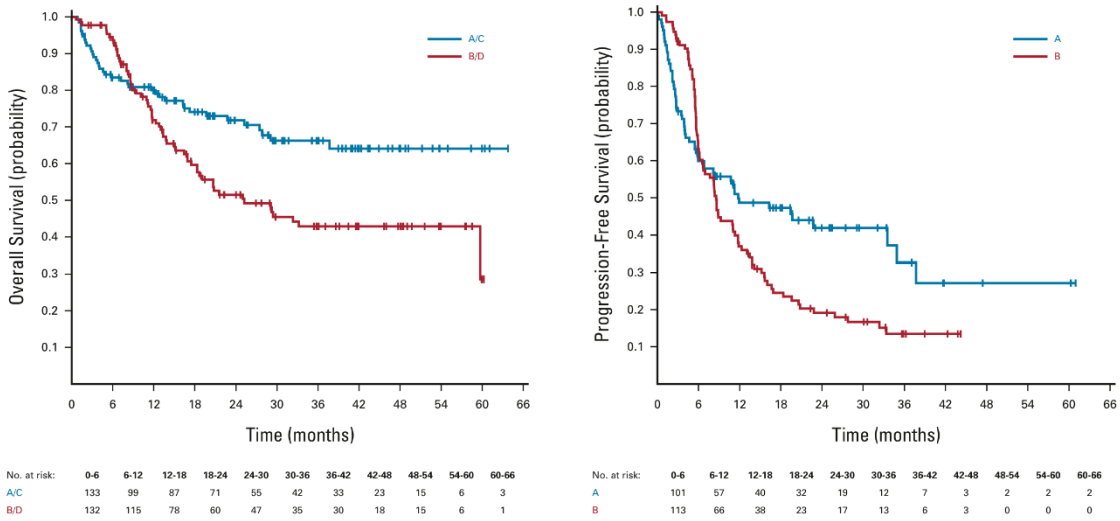

Figure 5. OS and PFS in patients treated with nivolumab-ipilimumab (arm A) or dabrafenib-trametinb (arm B). At disease progression, patients were enrolled to receive the alternate therapy: dabrafenib-trametinib (arm C) or nivolumab-ipilimumab (arm D). Kaplan-Meier curves were reproduced from The DREAMseq Trial[22].

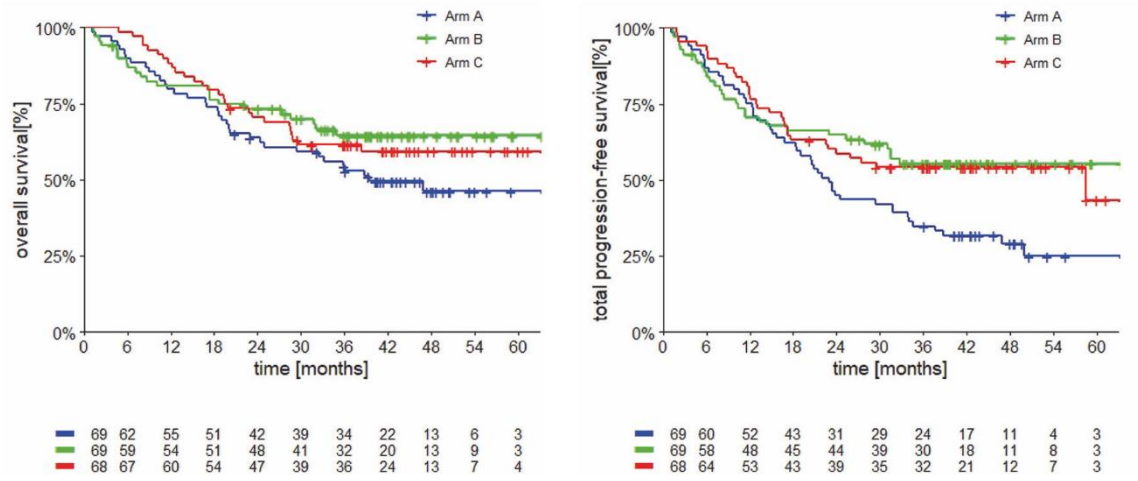

Figure 6. OS and PFS in patients who received encorafenib-binimetinib until PD followed by nivolumab-ipilimumab (arm A), nivolumab-ipilimumab until PD followed by encorafenib-binimetinib (arm B) or encorafenib-binimetinib for 8 weeks followed by nivolumab-ipilimumab until PD followed by encorafenib-binimetinib (arm C). Kaplan-Meier curves were reproduced from the phase II SECOMBIT trial[23].

1.3 Improving the efficacy of immunotherapy: Turning cold tumors into hot tumors

Early studies in colorectal cancer, notably those by Galon et al. in 2006, demonstrated that the density and spatial distribution of immune cells within the tumor microenvironment can predict prognosis and clinical outcomes. In particular, the presence of $CD8^+$ T cells with memory characteristics ($CD45RO^+$ $CCR7^+$) within the tumor core was shown to be a key determinant of survival[27]. This led to the conceptual distinction between "hot" (inflamed) and "cold" (immune desert) tumors. Initially, as described by Chen and Mellman, was proposed a three-way classification based on immune infiltration and T cell localization: immune-inflamed, immune-excluded and immune-desert[28]. This framework was later expanded by Galon's group, who introduced the Immunoscore, a classification system scoring from 0 to 14 based on the density of $CD3^+$ and $CD8^+$ T cells in both the tumor core and the invasive margin[29]. The Immunoscore in colorectal cancer has proven to be independent of T stage, N stage, age, sex, microsatellite instability (MSI) and other existing prognostic factors[30], although it has not yet been widely adopted in routine clinical practice. Further studies have shown that hot tumors are characterized by high tumor mutational burden (TMB), Abundant neoantigens and dense infiltration of T cells, PD-L1 expression, and regulatory T cells (Tregs)[31]. This is typical of tumors such as melanoma, non-small cell lung cancer (NSCLC), and MSI-high colorectal cancer which often originate from UV or smoking-induced mutational processes or defects in DNA repair pathways. In contrast, "cold" tumors display limited T-cell infiltration, low TMB, and are enriched in stromal components that generate a dense extracellular matrix. The immune infiltrate in these tumors is dominated by myeloid-derived suppressor cells (MDSCs), resulting in a profoundly immunosuppressive microenvironment (Figure 7)[31].

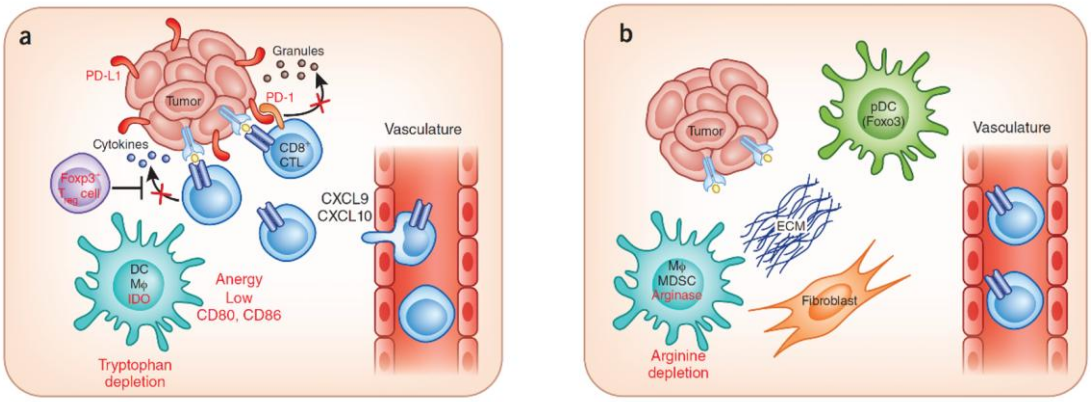

Figure 7. Immune regulatory pathways in T cell-inflamed vs. non-T cell-infiltrated tumors. (a) T cell-infiltrated tumors show chemokine-driven $CD8^+$ T cell recruitment, followed by functional inhibition via PD-L1, indoleamine 2,3-dioxygenase (IDO), Treg cells, and anergy mechanisms. (b) Non–T cell–infiltrated tumors lack chemokine expression and T cell presence, with immune suppression linked to stromal density and myeloid populations such as MDSCs and plasmacytoid dendritic cells (pDCs). Reproduced from Gajewski et al., 2013[31].

With the advent of immune checkpoint inhibitors (ICIs) in melanoma and other solid tumors, it has become evident that inflamed ("hot") tumors are more likely to respond to immunotherapy. These tumors evade immune surveillance primarily through the upregulation of checkpoint molecules such as PD-1 and PD-L1, yet they retain a pre-existing, antigen-specific T-cell response. Because these T cells are already present and functionally primed, blockade of the PD-1 pathway can restore their cytotoxic activity against tumor cells. This mechanism has translated into remarkable clinical outcomes: patients with metastatic disease, once deemed incurable, can now achieve complete and durable responses, with a subset effectively considered cured. This progress marks a paradigm shift in oncology, where metastatic cancer is no longer viewed solely as a chronic condition but as a potentially curable disease. This is not the case for "cold" tumors, which represent most solid malignancies and thus the greatest clinical challenge in immuno-oncology. Their paucity of T-cell infiltration and highly immunosuppressive microenvironment render checkpoint inhibitors largely ineffective. Consequently, a central goal for research is to convert cold tumors into hot ones. As we will discuss, several therapeutic strategies are under investigation with the main aim of inducing immunogenic cell death (ICD) and priming antitumor immune responses prior to the

initiation of checkpoint blockade, which would otherwise remain ineffective in the absence of pre-existing immunity.

1.3.1 Chemotherapy

In this context, cytotoxic chemotherapy, still the most established and effective treatment for many cancers, has been extensively investigated. While it is traditionally recognized for its immunosuppressive properties, particularly at high doses, numerous studies have revealed its potential to enhance antitumor immune responses. The pivotal mechanism is the induction of ICD: chemotherapy-induced damage to proliferating cancer cells leads to the release of tumor antigens and damage-associated molecular patterns (DAMPs), which are endogenous molecules released by damaged and dying cells. Tumor antigens are captured and processed by antigen-presenting cells (APCs), while DAMPs act as adjuvant "danger signals" that alert the immune system[32,33]. The most well-characterized DAMPs include the nuclear protein high mobility group box 1 (HMGB1), calreticulin, cytoplasmic double-stranded RNA (dsRNA), heat shock proteins (HSPs), and adenosine triphosphate (ATP) itself. These molecules ensure the presence of the two key components required to initiate an inflammatory response: antigen recognition plus an adjuvant signal. As a result, the induction of ICD can lead to a generalized inflammatory reaction. An additional well described mechanism that may further support this response is the ability of chemotherapy to upregulate MHC class I expression on tumor cells[34].
This association has already proven beneficial in clinical trials such as KEYNOTE-407, KEYNOTE-189, and CHECKMATE-9LA in NSCLC, and is already part of clinical practice.

1.3.2 Radiotherapy

Since 1953, when British radiologist Richard Mole first described the abscopal effect[35], a phenomenon referring to the regression of distant metastases outside the irradiated field, it became clear that radiotherapy could have systemic effects on the immune system[36]. Subsequent studies have confirmed that radiotherapy can also induce ICD and with the advent of ICIs, such reports have become increasingly prevalent. Indeed, preclinical models and clinical observations in patients with melanoma have demonstrated that focal radiation therapy can enhance systemic responses to immunotherapeutic antibodies[37,38].

Radiation therapy has also shown potential in eliciting abscopal effects in cases otherwise unresponsive to CTLA-4 blockade, although the clinical relevance of this phenomenon remains uncertain[39].

The mechanisms underlying this effect are similar to those observed with chemotherapy. Radiotherapy, too, can induce ICD and it has been shown to upregulate MHC class I expression on tumor cells[40] and promote the release of DAMPs. Moreover, radiation can enhance the emission of danger signals, including NKG2D ligands such as ULBP1 and RAET1G[41], as well as co-stimulatory molecules and death receptors[42]. However, although the immunogenic potential of radiotherapy is well established, the optimal dosing and fractionation strategies remain unclear. This uncertainty stems from conflicting results across different studies and experimental models.

The first randomized phase III clinical successful attempt to exploit this synergy was the PACIFIC trial in lung cancer[43], where the combination of radiotherapy plus immunotherapy proved superior to radiotherapy alone, with an estimated 5-year OS of 42.9% vs. 33.4% for durvalumab versus placebo[44]. Similarly, in limited-stage small cell lung cancer, the ADRIATIC trial showed that sequential addition of durvalumab to radiotherapy led to significantly longer OS than placebo (median-OS 55.9 months vs. 33.4 months)[45]. However, it is important to note the presence of negative studies on concomitant chemo-radiotherapy, such as KEYNOTE-412 in head and neck cancer[46]. This highlights the need to better understand dosage and fractionation, as not all regimens could be immunogenic. The timing of anti-PD1 administration, whether concurrent, sequential or pre/peri-radiotherapy also could play a critical role. Additionally, avoiding irradiation of lymph nodes could be considered, as they are key players in the generation of the immune response[47].

1.3.3 Interventional radiology

Interventional radiology techniques such as thermal ablation, radiofrequency ablation, transarterial chemoembolization (TACE), transarterial radioembolization (TARE), and percutaneous hepatic perfusion (PHP) have also been shown to induce ICD. However, as with radiotherapy, the optimal modality to elicit a robust immune response and the most effective timing for such interventions remain unclear[48]. Consequently, their use with the specific aim of modulating antitumor immunity is still limited in clinical practice. An

exception is represented by stage IV uveal melanoma with liver metastases, where liver-directed approaches are more frequently recommended, together with radiotherapy, often in conjunction with systemic immunotherapy[49,50].

Recently, the use of percutaneous techniques in metastatic uveal melanoma was supported by the FOCUS trial, originally designed as a randomized phase III study comparing melphalan (3 mg/kg every 6–8 weeks for up to six cycles) administered via PHP versus best alternative care, which included the investigator's choice of TACE, pembrolizumab, ipilimumab, or dacarbazine. Due to slow accrual and patient reluctance to randomization, the study was later amended to a single-arm design, ultimately enrolling 102 patients (95 treated with PHP). The trial reported an objective response rate (ORR) of 36.3%, a median progression-free survival (mPFS) of 9 months, and a median overall survival (mOS) of 20.5 months[51], leading to the approval of melphalan/PHP as the first FDA-approved liver-directed therapy for metastatic uveal melanoma.

The next step will be to design studies evaluating these percutaneous techniques in combination with immunotherapy. Early-phase investigations have already demonstrated the potential of such combinations to enhance systemic immune responses[52–54]. Therefore, even if the integration of interventional radiology into the field of immuno-oncology is still in its early stages, ultimately it appears highly promising. A key advantage of interventional radiology over systemic chemotherapy, and even over radiotherapy, is the ability to deliver very high drug concentrations directly to metastatic lesions with minimal systemic toxicity. Moreover, these techniques allow the local administration of virtually any agent, including immunomodulatory molecules capable of further amplifying the antitumor immune response and acting synergistically with systemic immunotherapy.

1.3.4 Oncolytic viral therapy

Oncolytic virus (OV) therapy employs viruses that are designed or selected to specifically infect malignant cells. Although well established in concept, it remains a challenging therapeutic strategy due to biological risks and the need for specialized facilities. Modern OVs are genetically engineered to infect and lyse tumor cells, leading to the release of DAMPs and tumor-associated antigens (TAAs), thereby eliciting an antitumor immune response that complements the direct oncolytic effect. Another key mechanism of action

involves the induction of type I interferon pathways. Viral components, typically viral RNA and DNA, are sensed by TLRs 3, 7, 8, and 9, while double-stranded RNA (dsRNA) is detected by RIG-I and MDA5, and viral dsDNA by the cytosolic DNA sensor cGAS. Activation of these innate immune receptors triggers a potent antiviral response that can convert the tumor into a “hot” immunogenic environment, thereby enhancing antitumor immunity.

At the beginning, pioneering studies by Alice Moore in the 1950s provided the initial proof of concept[55]. Early enthusiasm followed when the adenoidal–pharyngeal–conjunctival virus (now classified as adenovirus) induced extensive necrosis and hemorrhage within neoplastic tissues in clinical trials on cervix carcinoma[56]. However, these effects were only transient, as the virus was rapidly cleared by the host immune system, leading to no survival advantage. Moreover, occasional fatal neurotoxicity contributed to the abandonment of this approach. The advent of recombinant DNA technology revived the field by enabling the attenuation and precise engineering of viruses. This culminated in 2015 with the FDA approval for stage IV melanoma of the first oncolytic virus product, talimogene laherparepvec (T-VEC), based on a phase III trial showing a median-OS of 23.3 months compared with GM-CSF[57]. Nevertheless, with the introduction of ICIs, which provide substantially greater clinical benefit, T-VEC monotherapy has largely fallen out of use and the current rationale for OV therapy lies in priming the tumor microenvironment to enhance ICI efficacy. Indeed, phase II studies have begun to show preliminary signs of clinical benefit[58], though these remain limited at present.

Another promising approach to enhancing the immune response within the tumor microenvironment involves the modulation of cellular metabolism. As this represents the central focus of the present work, this concept will be explored in greater detail in the following section.

1.4 Metabolism and tumor microenvironment

In recent years, new insights in the field of immunometabolism have revealed a clear interconnection between metabolic pathways and the tumor microenvironment, which often proves hostile to immunotherapy. Tumor cells are highly metabolically active, as are activated anti-tumor immune cells. This creates a competitive dynamic for key metabolites, making nutrient restriction within the TME a great challenge for immune cells. Importantly, as we will explore, the suppression or redirection of metabolic processes not only affects immune cell function and viability but can also profoundly influence cellular differentiation. This can lead to dramatic shifts in immune cell behavior, whereby cells initially endowed with anti-tumor properties may acquire pro-tumoral functions[59].

1.4.1 Aerobic glycolysis and glutamine uptake

In highly proliferative and/or activated cells, the metabolic pathway of aerobic glycolysis is engaged. This term, coined by Otto Warburg in 1924, may seem counterintuitive but emphasizes the notion that, despite the presence of sufficient oxygen, these cells preferentially ferment pyruvate into lactate in the cytoplasm rather than channeling it into the tricarboxylic acid (TCA) cycle[60]. Initially, this preference was paradoxical, as glycolysis is energetically inefficient, yielding only 2 molecules of ATP per glucose molecule, in contrast to oxidative phosphorylation, which can generate up to 36 ATPs. The rationale became clearer later and as discussed by Vander Heiden et al., lay in the fact that only through sustained activation of glycolytic flux a proliferating tissue can generate the full spectrum of metabolites required to support biomass accumulation and cell division. Moreover, inefficient ATP production is not necessarily detrimental in the context of continuous nutrient supply via the bloodstream and studies on actively proliferating cells have shown that those relying on aerobic glycolysis maintain high ATP/ADP and $NADH/NAD^+$ ratios[61]. These findings suggest that aerobic glycolysis is not a consequence of defective respiration, but rather a regulated metabolic state that supports the biosynthetic demands of proliferation. Indeed, the accumulation of glycolytic intermediates enables several critical biosynthetic pathways, including the pentose phosphate pathway (PPP), hexosamine biosynthesis, the conversion of dihydroxyacetone

phosphate (DHAP) into glycerol-3-phosphate, and the use of 3-phosphoglycerate for the synthesis of serine, glycine, and methyl donors, as well as NADPH[62] (Figure 8). Importantly, in proliferative cells such as tumor cells and activated T cells, oxidative phosphorylation (OXPHOS) is also upregulated compared to their naive state. This is because citrate must be actively exported to the cytoplasm and converted into acetyl-CoA to meet the high demand for fatty acid and cholesterol synthesis required for membrane biogenesis.

Another characteristic of proliferating tissues is the increase of glutamine uptake to support nucleotides, amino acids and fatty acid synthesis. To sustain this high demand for biomass production, TCA intermediates such as oxaloacetate (OAA) α-ketoglutarate and citrate are diverted from Krebs cycle and, because these intermediates are depleted, anaplerotic reactions become essential to replenish the TCA cycle that otherwise would stop[62]. In this context, the increase of glutamine uptake via transporters such as SLC1A5, SLC38A1/SLC38A2, and LAT1 plays a central role[63]. In facts, the conversion of glutamine into α-ketoglutarate through glutaminolysis, sustain TCA cycle activity. Furthermore, glutamine contributes to lipid synthesis by supplying carbon (via mitochondrial OAA) for citrate production and by generating NADPH through its conversion to lactate[64]. This critical role of glutamine for cell proliferation, as first demonstrated by Harry Eagle in the 1950s[65], is underscored by the fact that all standard cell culture media require 10- to 100-fold molar excess of glutamine relative to other amino acids.

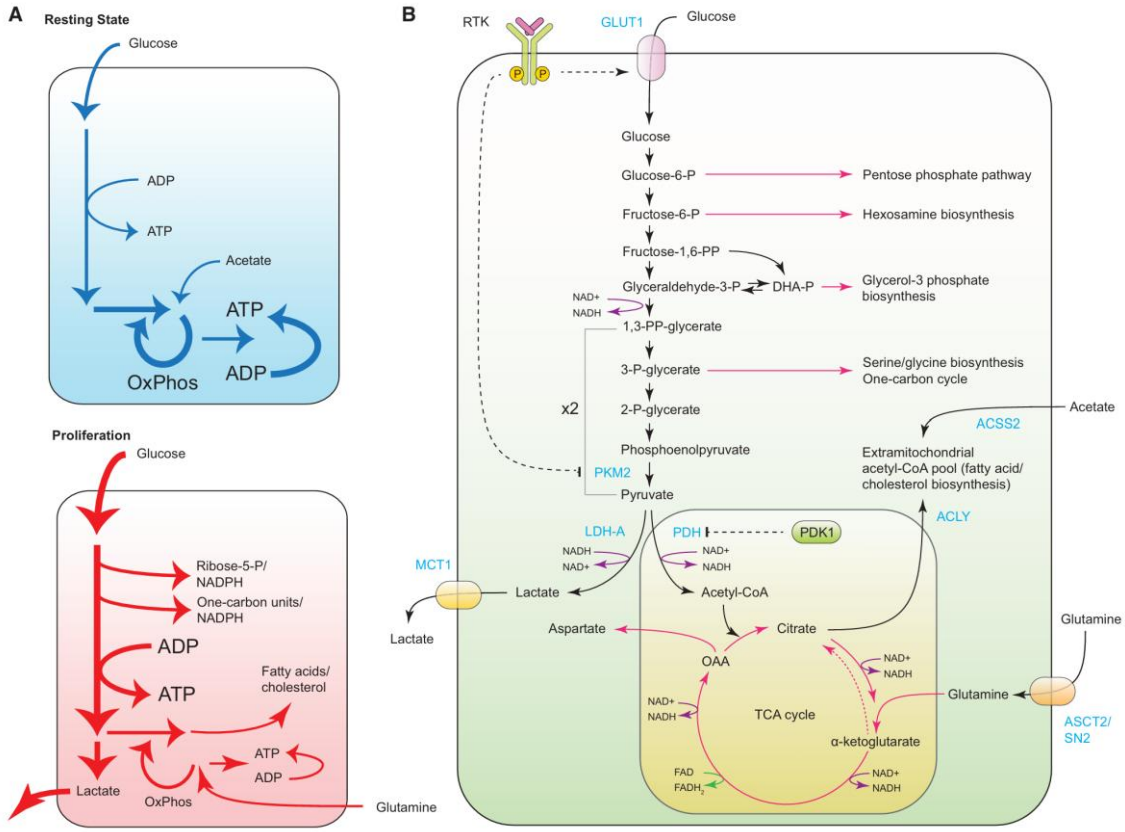

Figure 8. Glycolysis and TCA cycle intermediates in resting vs. proliferating cells.
(A) Resting cells primarily use glucose and acetate for oxidative phosphorylation to generate ATP. In contrast, proliferating cells divert glucose into biosynthetic pathways for nucleotide, lipid, and amino acid synthesis, alongside lactate production. (B) Glucose metabolism supports diverse biosynthetic outputs via glycolysis and the TCA cycle, including the pentose phosphate pathway, serine/glycine synthesis, and fatty acid/cholesterol biosynthesis. Key transporters and enzymes include GLUT1, LDH-A, PDH, ACLY, and ACSS2.
RTK, receptor tyrosine kinase; GLUT1, glucose transporter 1; MCT1, monocarboxylate transporter 1; ASCT2/SN2, glutamine transporter; PKM2, pyruvate kinase M2; LDH-A, lactate-dehydrogenase A; PDH, pyruvate dehydrogenase; ACLY, ATP-citrate lyase; ACSS2, acetyl-CoA synthetase 2. Reproduced from Pavlova et Thompson, 2016[62].

1.4.2 Lipid and cholesterol biosynthesis

In healthy humans, de novo fatty acid (FA) biosynthesis is essentially restricted to the liver, the adipose tissue, and the lactating breast[66]. However, as demonstrated by Medes et al. in 1953, tumors synthesize lipids at a rate comparable to that of the liver[67]. FA synthesis has been extensively documented across various cancer types, and multiple studies have confirmed that lipogenesis is essential for tumor growth[68]. Importantly, these lipids are not only used for membrane synthesis but also serve as substrates for FAO to fuel OXPHOS. Thus, it is not surprising that lipogenesis and FAO are simultaneously active in cancer cells. The central precursor for FA synthesis is cytosolic acetyl-CoA, which accumulates in cancer and proliferating cells through the metabolism of glucose, acetate, and glutamine. Next, its transformation into malonyl-CoA mediated by Acetyl-CoA carboxylase (ACC) drives the reactions towards fatty acids synthesis and eventually the multi enzyme complex fatty acid synthase (FASN) catalyze the condensation of seven malonyl-CoA molecules and one priming acetyl-CoA generating palmitate, a 16-carbon saturated FA (16:0) which is the initial product of FA synthesis[69]. From this molecule, through reactions of elongation and desaturation cells will generate the non-essential lipid molecules that need to sustain replication.

The expression of enzymes involved in FA biosynthesis is regulated by sterol regulatory element-binding proteins (SREBPs), a family of three basic helix–loop–helix–leucine zipper (bHLH-LZ) transcription factors: SREBP1a and SREBP1c (splice variants of the *SREBF1* gene), and SREBP2 (encoded by *SREBF2*). While SREBP1c primarily induces genes involved in FA metabolism, SREBP2 activates genes of the mevalonate (MVA) pathway, and SREBP1a regulates both pathways[70].

Similarly to fatty acids, cholesterol is an essential component of eukaryotic cell membranes, comprising up to 30% of membrane content, although its distribution varies across cellular compartments. Cholesterol's polar hydroxyl group interacts with the polar heads of phospholipids and sphingolipids, contributing not only to membrane structure but also to fluidity, protein mobility, cell signaling, and intracellular trafficking[71]. Importantly, cholesterol is concentrated in membrane microdomains known as lipid rafts, which facilitate the formation of signaling complexes by clustering receptors and second messengers[72].

Hence, to meet the demands for rapid proliferation, proliferative cells also need to upregulate genes of MVA pathway, the metabolic route responsible for cholesterol biosynthesis. This is achieved through activation of SREBP2 and concurrent inhibition of liver X receptors (LXRα and LXRβ isoforms)[73]. SREBP2 promotes transcription of MVA pathway enzymes, including 3-Hydroxy-3-Methylglutaryl-CoA Reductase (HMGCR), the rate-limiting enzyme. Additionally, SREBP2 enhances cholesterol uptake by inducing low-density lipoprotein receptor (LDLR) expression. In contrast, LXRs promote reverse cholesterol transport (RCT) by upregulating ABCA1 and ABCG1, which facilitate cholesterol efflux to the liver. The elegant mechanism that regulates SREBP2 and LXR activity resides in the endoplasmic reticulum (ER) and involves SREBP cleavage-activating protein (SCAP) and insulin-induced gene (INSIG). Under high cholesterol conditions, the SREBP-SCAP complex binds to INSIG, retaining it in the ER and preventing SREBP2-mediated cholesterol synthesis. This retention is mediated by the binding of 25/27-Hydroxycholesterol (25/27-HC) to INSIG and/or cholesterol and desmosterol to SCAP (Figure 9)[71,74]. Additionally, cholesterol and desmosterol bind to LXR heterodimers, promoting LXR-mediated RCT. Conversely, when cholesterol levels are low, INSIG dissociates from the SREBP-SCAP complex, which is then escorted by COPII vesicles to the Golgi. There, SREBP undergoes sequential proteolytic cleavage by Site-1 (S1P) and Site-2 (S2P) proteases, allowing its nuclear translocation and the consequently activation of cholesterol biosynthesis[75]. Under these conditions, LXRs remain transcriptionally repressed.

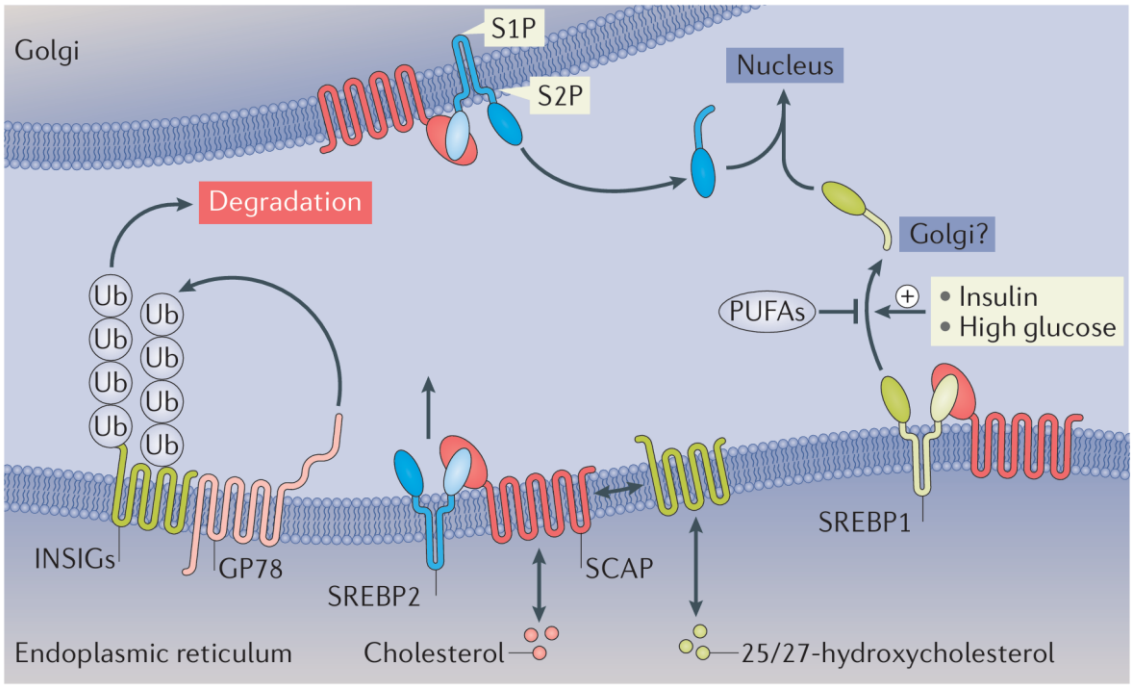

Figure 9. Regulation of SREBP activation. SREBP2 activation is inhibited by cholesterol and oxycholesterols (25/27-hydroxycholesterol), which retain the SCAP-SREBP2 complex in the endoplasmic reticulum via INSIGs. In sterol-depleted conditions, INSIGs become ubiquitylated (Ub) and are rapidly degraded, allowing SCAP-SREBP2 transport to the Golgi, where SREBP2 is cleaved by S1P and S2P to release its active domain. SREBP1 activation is less dependent on sterols and is modulated by polyunsaturated fatty acids (PUFAs), insulin, and glucose. SREBP1 activation remains incompletely understood. GP78, E3 ubiquitin-protein ligase autocrine motility factor receptor (AMFR). Reproduced from Shimano and Sato, 2017[75]. License number: 6156010808606.

Besides its fundamental role in cholesterol biosynthesis, MVA pathway is also essential for the production of isoprenoids and other sterol molecules fundamental for proper cellular function. It utilizes the same core substrates as fatty acid synthesis (acetyl-CoA, NADPH, and ATP) and is tightly integrated into the overall metabolic state of cancer cells. As illustrated in Figure 10, the diversion of acetyl-CoA into the MVA pathway enables proliferating cells to synthesize key intermediates such as farnesyl pyrophosphate (FPP) and geranylgeranyl pyrophosphate (GGPP). These metabolites are generated through the sequential condensation of dimethylallyl diphosphate with two or three units of isopentenyl diphosphate (IPP), respectively. The hydrophobic chains of FPP and GGPP are crucial for the post-translational isoprenylation of proteins, a modification that anchors them to cellular membranes and ensures correct subcellular localization and

function[76]. Notably, small GTPases of the Ras and Rho families, require isoprenylation to regulate signal transduction and cytoskeletal dynamics effectively.

In vitro experiments have demonstrated that pharmacological inhibition of HMG-CoA reductase (HMGCR) by statins disrupts the MVA pathway, resulting in cell rounding, disassembly of actin stress fibers, G1-phase cell cycle arrest, and increased apoptosis. These effects are reversed by supplementation with GGPP, and in some cases FPP, underscoring their critical role in tumor cell viability[77,78]. Evidence suggests that no single isoprenylated protein is solely responsible for this dependency; rather, it represents a broader "class effect," wherein depletion of isoprenoid pools affects numerous isoprenylated proteins simultaneously[76].

Other metabolites derived from MVA pathway activation include dolichol and coenzyme Q (CoQ). Dolichol is a long-chain lipid molecule composed of approximately 18-20 IPP units and localized to the ER membrane, where it plays an essential role in N-linked glycosylation of nascent proteins[79]. N-glycosylation is crucial for proper protein folding and activity, as shown by findings that the absence of SCAP N-glycosylation keeps the SCAP-SREBP complex inactive in the ER, even under low-sterol conditions[80]. Isoprenoids are also utilized for the biosynthesis of CoQ. The hydrophobic isoprenoid tail anchors CoQ within the inner mitochondrial membrane, enabling the quinone moiety to transfer electrons from complexes I and II to complex III of the electron transport chain, thereby sustaining oxidative phosphorylation and ATP production[81].

The importance of the MVA pathway and its metabolites in cancer biology is underscored by the convergence of classical oncogenic and proliferative signaling cascades, such as PI3K-AKT, mTORC1, AMPK, TP53, RB, and MYC, on this metabolic route. As reviewed by Mullen et al., these pathways cooperate through diverse mechanisms to establish a strong functional link between oncogenic signaling and metabolic reprogramming[76].

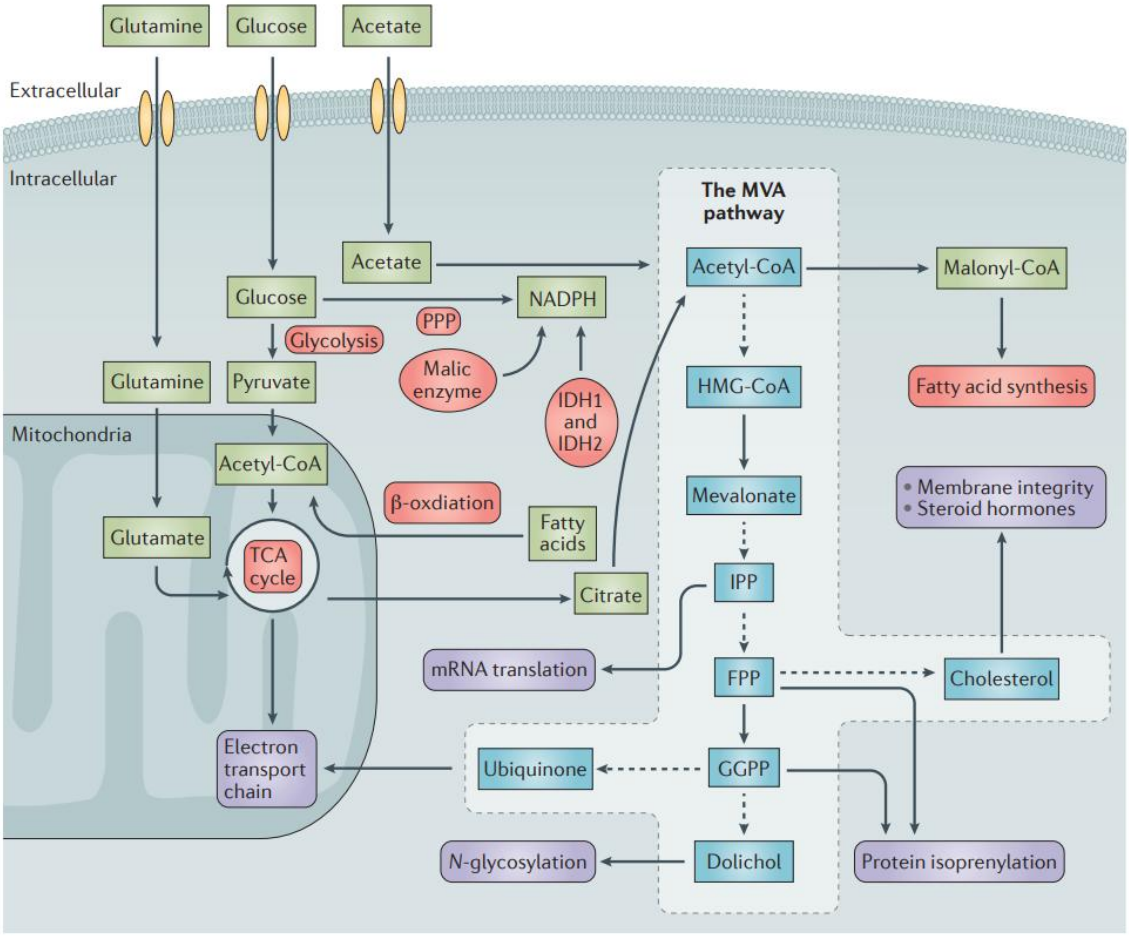

Figure 10. Schematic representation of the metabolic steps leading from acetyl-CoA to cholesterol, isoprenoid intermediates, and downstream biological functions. The figure illustrates the integration of glucose, glutamine and acetate metabolism with the MVA pathway. HMG-CoA, 3-hydroxy-3-methylglutaryl CoA; IPP, isopentenyl-diphosphate; FPP, farnesyl diphosphate; GGPP, geranylgeranyl-diphosphate; IDH, isocitrate dehydrogenase; PPP, pentose phosphate pathway; TCA cycle, tricarboxylic acid cycle. Reproduced from Mullen et al., 2016[76]. License number: 6155981238041.

1.5 Impact of TME metabolic reprogramming on immune cells function

The metabolic circuits described above shape four key features of the TME: glucose deprivation, hypoxia, acidosis and amino acid depletion (Figure 11). As already stated, they contribute to establishing a competitive challenge for nutrients among TME-resident cells. The resulting nutrient restriction not only impairs cellular function and viability but also generates profound phenotypic changes. Immune cells initially programmed for antitumor activity may undergo functional reprogramming, acquiring immunosuppressive and pro-tumoral properties[59].

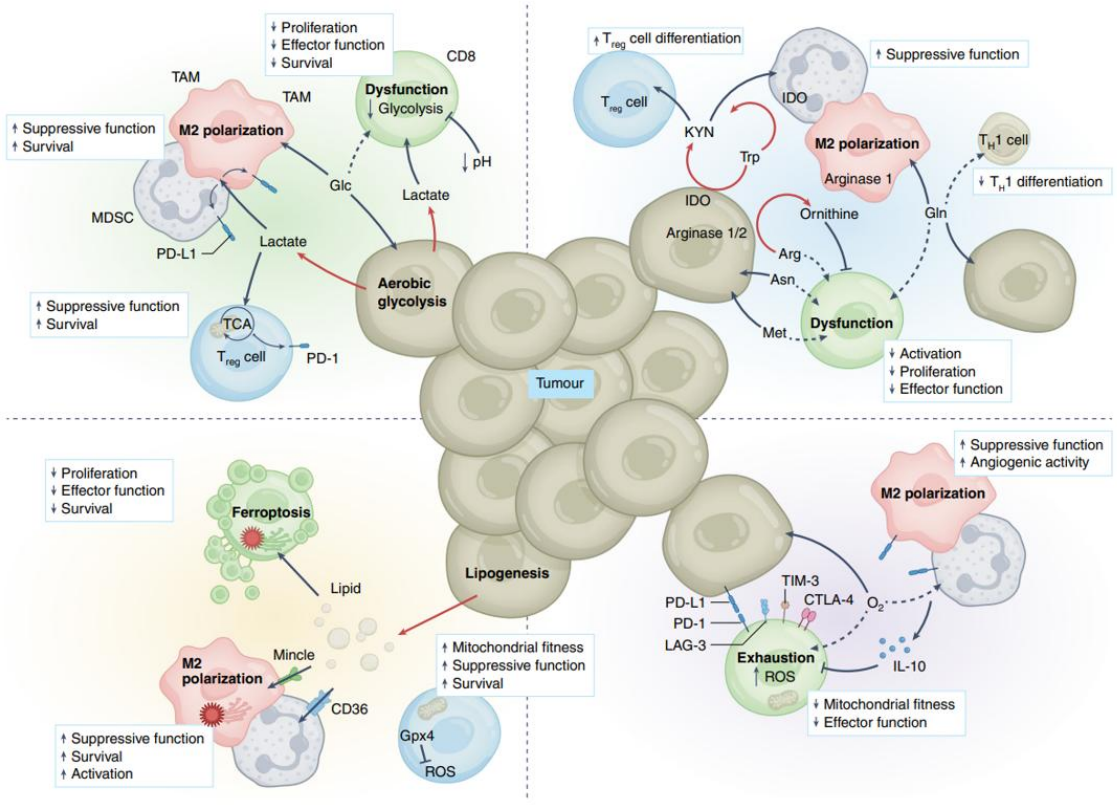

Figure 11. Key metabolic alterations within the tumor–immune microenvironment and their impact on immune cell function. Reproduced from Kao et al., 2022[59]. License number: 6156011132205.

Among immune system cells, T cells have been the most extensively studied in terms of how these metabolic constraints within the TME affect their function. When combined with chronic antigen stimulation, these metabolic stressors contribute to T cell exhaustion, a dysfunctional state characterized by the upregulation of inhibitory receptors such as PD-

1, LAG-3, and TIM-3, along with reduced proliferative capacity and impaired cytokine production[82]. Glucose deprivation leads to a reduction of the glycolytic activity, which is directly linked to cytokine synthesis. The enzyme GAPDH, when not engaged in glycolysis, has been shown to bind the mRNA of IFN-γ preventing its translation[83], whereas inhibition of LDHA results in reduced production of key cytokines including IFN-γ itself[84]. Consequently, enhancing glycolytic flux in T cells has been associated with improved anti-tumor efficacy[85]. Glucose availability also influences T cell fate. For instance, inhibition of mTOR complex 1 signaling with rapamycin[86] or direct blockade of glycolysis using 2-deoxyglucose, which targets hexokinase 2[87], have been shown to promote the development of memory T cells. mTOR complex 2 has also been implicated in this process[88]. However, it is important to note that these findings are primarily based on in vitro studies, and it remains unclear whether similar metabolic interventions can induce memory phenotypes in vivo.

Both acidosis and hypoxia are also known to impair $CD8^+$ T cell function. Acidosis inhibits nuclear translocation of nuclear factor of activated T cells (NFAT)[89], dampening T cell activation, mitochondrial fitness, and effector cytokine production. The effects of hypoxia are less clear. On the one hand, hypoxia-driven activation of HIF-1α is required for glycolytic reprogramming and cell survival[90] and leads to enhanced cytotoxic and antitumor activity in adoptive transfer models of $CD8^+$ T cells cultured under hypoxic conditions[91]. On the other hand, several in vivo studies have shown that a chronically hypoxic tumor microenvironment generally contributes to functional impairment of T cells under sustained stress[92]. This apparent discrepancy may be partly explained by the heterogeneous distribution of hypoxic regions within tumors, which also makes it difficult to establish reliable experimental systems.

Amino acid deprivation further exacerbates T cell dysfunction within the TME. Beyond the elevated glutamine consumption by tumor cells, immunosuppressive enzymes such as indoleamine 2,3-dioxygenase (IDO) and arginase-1 (ARG1), expressed predominantly by M2-polarized macrophages and MDSCs, deplete essential amino acids like tryptophan and arginine, which are critical for T cell survival and effector function[93,94]. Moreover, the enzymatic products kynurenine and polyamines have been shown to exert potent immunosuppressive effects[95].

Notably, while these metabolically adverse conditions impair the function of effector $CD8^+$ T cells, regulatory $CD4^+$ T cells (Tregs) exhibit a remarkable capacity to adapt to the TME[96]. Tregs predominantly rely on fatty acid oxidation (FAO) and OXPHOS to meet their energetic demands[97], enabling them to persist and function effectively in nutrient-deprived, hypoxic, and acidic settings. This metabolic resilience fosters a self-perpetuating cycle of immunosuppression, wherein the same environmental constraints that hinder anti-tumor immunity simultaneously promote the survival and activity of immunosuppressive cell populations. This phenomenon also extends to myeloid cells, although their metabolic regulation remains comparatively less explored. The activation and maturation of key anti-tumor myeloid populations, such as dendritic cells (DCs) and classically activated M1 macrophages, are intrinsically dependent on aerobic glycolysis. For instance, enforced activation of OXPHOS via AMP-activated protein kinase (AMPK) has been shown to inhibit DC maturation[98] as well as nitric oxide (NO), a hallmark effector molecule produced by M1 macrophages, promotes glycolysis while simultaneously suppressing mitochondrial respiration through direct inhibition of respiratory complexes[99]. It is well documented that the metabolic landscape of the TME profoundly interferes with the maturation of myeloid cells, which consequently remain trapped in an immature, immunosuppressive state known as MDSCs. Tumor-derived factors such as VEGF, GM-CSF, and IL-6 disrupt physiological myelopoiesis, resulting in the premature release of these immature myeloid cells into circulation[100,101]. Like Tregs, MDSCs rely predominantly on OXPHOS and are metabolically adapted to persist in glucose-depleted, hypoxic, and acidic environments[102]. Consistent with this, they exhibit increased fatty acid catabolism, which sustains their survival and immunosuppressive functions. In these cells polyunsaturated fatty acid–containing phospholipids (PUFA-PLs) are particularly relevant. Heightened mitochondrial FAO, together with the avid uptake of PUFAs from the TME, leads to their intracellular accumulation. This, in turn, promotes redox imbalance driven by reactive oxygen species (ROS)–generating pathways, triggering ferroptotic stress and ultimately ferroptotic cell death[103]. Notably, ferroptosis itself has been shown to convert neutrophils into highly immunosuppressive polymorphonuclear MDSCs (PMN-MDSCs)[104]. Moreover, lipid peroxidation products released during this process further suppress T-cell activity and can induce ferroptosis in macrophages, reinforcing a self-perpetuating immunosuppressive

loop[104]. Comparable mechanisms of aberrant lipid accumulation have been described in other myeloid populations. For instance, in DCs, excessive intracellular lipids impair antigen presentation[105], through mechanisms such as heat-shock protein 70 (HSP70)-mediated interference and reduced surface expression of MHC class I molecules[106]. Similarly, the uptake of oxidized lipids from the TME contributes to DC dysfunction and loss of immunostimulatory capacity[107] while tumor-associated macrophages (TAMs) exhibit elevated CD36 expression, driving lipid accumulation and polarization toward an M2-like, pro-tumoral phenotype[108].

1.6 Mevalonate pathway, isoprenoids synthesis and immune response

It is becoming increasingly clear that MVA pathway, which regulates the biosynthesis of cholesterol, also exerts important immunomodulatory functions. This concept is well exemplified by the human genetic disorder mevalonate kinase deficiency (MKD), caused by loss-of-function mutations in the *MVK* gene. MKD gives rise to two clinical phenotypes that actually represent a continuous spectrum of disease severity: the milder form, Hyper-IgD Syndrome (HIDS), characterized by recurrent febrile episodes, lymphadenopathy, arthralgia, skin rash, and elevated serum IgD levels; and the more severe form, mevalonic aciduria (MA), which presents with encephalopathy, dysmorphic features, psychomotor delay, and profound inflammatory dysfunction[109].

The mechanistic basis of this pro-inflammatory phenotype remains a matter of debate. It is still not known with certainty whether the inflammatory response arises from the blockade of cholesterol biosynthesis itself or from the inhibition of isoprenoid synthesis, one of several essential intermediates of the MVA pathway. As discussed before, in addition to cholesterol, MVA pathway gives rise to a variety of crucial intermediates collectively known as isoprenoids, including GGPP and FPP. These molecules are required for the post-translational modification and activation of small GTPases. GGPP is critical for the activity of Rho family proteins, whose function depends on geranylgeranylation mediated by geranylgeranyltransferase I (GGTase-I). In this context, Khan et al. demonstrated that mice lacking GGTase-I specifically in macrophages develop severe autoimmune joint inflammation resembling erosive rheumatoid arthritis. Mechanistically, macrophages from these mice accumulated high levels of active GTP-bound RAC1, CDC42, and RHOA, with RAC1 remaining associated with the plasma

membrane, indicative of sustained activity. Moreover, GGTase-I deficiency triggered the activation of p38-MAPK and NF-κB pathways and enhanced the production of proinflammatory cytokines[110]. Subsequently, Park et al. elucidated how dysregulation of RhoA due to impaired prenylation may represent the molecular connection between MKD and another well-documented autoinflammatory disorder, the familial Mediterranean fever (FMF), which is caused by mutations in the MEFV gene encoding pyrin. In fact, active RhoA negatively regulates the pyrin inflammasome, whereas treatment with simvastatin, which depletes isoprenoid intermediates and thereby inhibits RhoA prenylation causing its translocation from the plasma membrane to the cytosol, induces a dose-dependent release of IL-1β from LPS-primed bone marrow-derived macrophages[111]. Furthermore, the loss of GGTase-I in macrophages altered the interaction between KRAS and the PI3K catalytic subunit p110δ, thereby impairing PI3K activation. This disruption resulted in a hyperinflammatory state characterized by uncontrolled TLR signaling and constitutive activation of the pyrin inflammasome[112]. Geranylgeranylation can also play important roles in antigen presentation. In fact, in a study by Xia et al., inhibition of the MVA pathway using statins administered as vaccine adjuvant resulted in markedly improved antitumor vaccination efficacy and synergist effect when combined with anti-PD1 antibodies. They demonstrated that statin therapy impaired Rab5 function, ultimately leading to arrested endosomal maturation, prolonged antigen retention and consequently enhanced antigen presentation and T cell activation[113].

In addition to the isoprenylation of small GTPases, cholesterol content of cell membranes itself can modulate immune cell activation, differentiation, and proliferation. Elevated membrane cholesterol has been associated with increased expression of inhibitory receptors such as PD-1, 2B4, TIM-3, and LAG-3 in $CD8^+$ tumor-infiltrating lymphocytes. Notably, after homing to the tumor site, $CD8^+$ T cells accumulate cholesterol, which triggers the upregulation of the ER stress response genes, particularly XBP1. This, in turn, directly drives the transcription of immune checkpoint molecules. Importantly, inhibition of XBP1 or reduction of intracellular cholesterol levels in $CD8^+$ T cells effectively restores their antitumor activity[114]. In this setting, Bensinger et al. provided an elegant mechanistic link between T cell activation and cholesterol metabolism. They showed that during activation, T lymphocytes upregulate the oxysterol-metabolizing enzyme SULT2B1, resulting in suppression of LXR target genes and the concurrent activation of

the SREBP-2 pathway, which drives cholesterol biosynthesis. This metabolic reprogramming confers a proliferative advantage and enhances antigen-driven T cell response[73]. Furthermore, TCR engagement itself can activate SREBP-2 signaling and activated T cells from Scapfl/fl mice, which are unable to activate SREBP, fail to acquire the aerobic glycolytic metabolism required for proliferation and effector functions. Compared with wild-type counterparts, activated Scapfl/fl T cells exhibit markedly reduced survival, proliferation and ER expansion accompanied by 50% less cellular cholesterol content. Remarkably, supplementation with exogenous cholesterol restored these defects, underscoring that intracellular cholesterol acts as a critical metabolic checkpoint governing cell-cycle progression through regulation of ER membrane biogenesis[115]. Cholesterol regulation and distribution have a fundamental role also in innate immune cells. It was recently described that interferon signals in macrophages mediate a rapid movement of specific pools of cholesterol in plasma membrane (without change in total cholesterol level) conferring resistance to Gram-positive cholesterol-dependent cytolysins. The redistribution of cholesterol requires coordinated inhibition of new cholesterol synthesis, increase in cholesterol esterification and the endogenous production of 25-HC by cholesterol 25-hydroxylase[116].

In addition to the Pyrin inflammasome previously mentioned, sterol depletion or pharmacological inhibition of cholesterol synthesis with statins can trigger inflammatory responses in macrophages and dendritic cells via activation of the NLRP3 inflammasome. It has been shown that this mechanism relies on the translocation of a ternary complex composed of SREBP2, SCAP and NLRP3 from the endoplasmic reticulum to the Golgi apparatus, rather than simply changes in total cholesterol levels[117]. Conversely, other studies provide complementary evidence that intracellular cholesterol accumulation in antigen-presenting cells enhances NLRP3 inflammasome activation and promotes pro-inflammatory responses[118,119]. Together, these data suggest that both dysregulation of cholesterol biosynthesis/trafficking and excessive cholesterol accumulation converge on NLRP3 activation through distinct but related mechanistic pathways.

Overall, these findings highlight the intimate connection between cholesterol metabolism and immune regulation and underscore the need for further investigation into the potential therapeutic implementation of cholesterol-modulating agents in cancer immunotherapy. In the following section, we will discuss the clinical evidence accumulated to date on the

antitumor effects of statins, a widely prescribed class of cholesterol-lowering agents that inhibit HMGCR, and their potential synergy with immune checkpoint inhibitors.

1.7 Statins and cancer: from epidemiological studies to the emerging evidence in immunotherapy

Before the advent of immunotherapy, the impact of hypercholesterolemia and statin use on carcinogenesis and cancer prognosis had been extensively investigated through numerous long-term epidemiological studies. In line with the landmark population-based study by Nielsen et al. published in 2012, which analyzed 295.925 Danish patients diagnosed with cancer between 1995 and 2007, demonstrating that statin use was associated with an approximately 15% reduction in cancer-related mortality with an adjusted hazard ratio (HR) of 0.85 across several tumor types[120], several large retrospective cohorts described similar associations between statin exposure and improved cancer outcomes[121–125]. However, many other investigations failed to confirm these findings[126,127]. Beyond the inconsistency of these results, the interpretation of positive associations is substantially limited by several sources of bias inherent to retrospective observational studies. These include healthy user bias, whereby statin users are more likely to engage in health-seeking behaviors and receive closer medical surveillance; confounding by indication, as statins are preferentially prescribed to patients with a better baseline prognosis or longer life expectancy; immortal time bias, which may artificially inflate survival estimates if statin exposure is defined after cancer diagnosis; and residual confounding, due to incomplete adjustment for comorbidities, socioeconomic status, lifestyle factors, and concomitant medications. In addition, heterogeneity in cancer types, disease stages, statin class, dosage, duration of exposure, and study endpoints, together with publication bias favoring positive results, further limits the robustness and comparability of these analyses[128,129].

Randomized controlled trials conducted for cardiovascular indications offer greater methodological rigor and are largely less susceptible to these biases. Nevertheless, these studies, have consistently shown no significant association between statin use and cancer incidence or mortality[130], a conclusion also endorsed by the American Heart Association[131]. Importantly, these trials were not designed to evaluate oncologic endpoints, and their duration and follow-up may have been insufficient to capture

potential effects on tumor development or progression. Overall, no definitive conclusion could be drawn.

In this context, the only reliable approach to clarify the potential causal relationship between statin use and cancer outcomes is through randomized controlled trials specifically designed to address the question. Among the few oncology-dedicated randomized studies conducted to date, the LUNGSTAR (pravastatin 40 mg with chemotherapy in small-cell lung cancer)[132], the PRO-STAT (adjuvant low-dose atorvastatin after prostatectomy)[133], and a simvastatin plus chemotherapy trial in metastatic/locally advanced breast cancer[134] have all yielded negative results. A large, ongoing phase III trial, the MASTER study, evaluating high-dose atorvastatin (80 mg) in combination with standard therapy for early-stage ER-positive breast cancer, has been specifically designed to address this issue and is expected to provide clearer insights into the role of statins in cancer therapy.

In the meantime, since FDA approval of ipilimumab in 2011, immune checkpoint inhibition has revolutionized cancer therapy, leading to regulatory approvals across a broad range of solid malignancies. This rapid expansion of immunotherapy use has, in turn, prompted a new wave of retrospective studies exploring the association between statin therapy and oncologic outcomes in patients treated with immune checkpoint inhibitors (ICIs). Such analyses may provide valuable insights into the clinical contexts in which concomitant statin use could confer the greatest benefit[135]. In fact, recent evidence indicates that statins may enhance the responsiveness to PD-1 blockade. Several retrospective studies and meta-analyses conducted to date have consistently reported improved outcomes in statin users treated with ICIs across various cancers[136]. For example, in metastatic renal cell carcinoma, Santoni et al. found that patients receiving ICI-based combinations with concomitant statins had significantly longer overall survival (HR = 0.48) and higher overall clinical benefit compared with statin non-users[137]. Similar findings were observed in thoracic malignancies: Cantini et al. reported longer PFS (6.7 vs. 2.9 months) and OS (13.1 vs. 8.7 months), and higher ORR (32% vs. 18%) among statin users with malignant pleural mesothelioma or NSCLC treated with PD-1 inhibitors[138]. In line with this, Rossi et al. described superior median-PFS, median-OS, and ORR in statin users, particularly in patients with PD-L1 expression <50%, suggesting a possible interaction with the immune tumor microenvironment[139]. Large real-world

analyses by Cortellini et al. and Marrone et al. further confirmed these associations, showing improved ORR[140] and overall mortality[141]. As with the studies discussed above, these analyses are observational and retrospective and, although carefully conducted with multivariable analyses included, remain affected by the same sources of bias. Nevertheless, given the strong rationale previously discussed correlating MVA pathway inhibition to immune activation, we believe that, in combination with immunotherapy, this could represent the most appropriate setting in which to evaluate statin therapy in cancer, warranting further investigation.

Chapter 2

AIMS OF THE STUDY

The first aim of this study is to determine whether statin therapy enhances the clinical efficacy of immune checkpoint inhibitors (ICIs) in patients with metastatic melanoma. To address this aim, we shall evaluate clinical outcomes in a cohort of patients treated with anti-PD1 therapy, assessing whether concomitant statin use correlates with improved progression-free and overall survival. Furthermore, we shall validate these observations by using a murine melanoma model.

The second aim is to elucidate the mechanistic basis of statin-ICI interaction. To address this aim, we shall perform in vivo and in vitro experiments. In vivo, we shall evaluate the immune landscape of tumor-infiltrating cells to analyze and quantify immune subsets differently present in simvastatin-treated tumor-bearing mice. In vitro, we shall treat with simvastatin immune cells identified in vivo to recapitulate the same phenotypic changes identified in vivo, and to characterize the molecular mechanism(s) underlying simvastatin activity.

Chapter 3

MATERIALS AND METHODS

3.1 Patient characteristics and survival analysis

The clinical characteristics of patients with melanoma are described in Table 2. Peripheral Blood Mononuclear Cells (PBMCs) were collected after signing written informed consent (Prot. N° 12/23 oss. approved by Istituto Nazionale Tumori IRCCS Fondazione "G. Pascale", Naples, Italy, and MTA between Istituto Nazionale Tumori IRCCS Fondazione "G. Pascale" and IRCCS Scientific Institute San Raffaele, Milan, Italy for samples transfer). Median-PFS and median-OS were evaluated using the Kaplan-Meier method. Statistical significance between the survival curves was assessed using log-rank test to assess statistical significance. Cox proportional hazards regression was used for multivariate analysis of PFS and OS, and to compute the hazard ratios (HRs) for disease progression and death with 95% CIs. To determine the covariates for the multivariate analysis, a preliminary univariate analysis was conducted on all covariates. The selection of variables was based on their HRs or their clinical relevance. Fisher's exact test was used to evaluate the association between statin use and objective response rate (ORR). An alpha level of $p < 0.05$ was considered statistically significant for all analyses. Statistical computations were conducted using IBM SPSS (Statistical Package for the Social Sciences) and MedCalc Statistical Software. PFS was defined as the length of time from treatment initiation to disease progression or death. OS was defined as the length of time from treatment initiation to death. ORR was defined as the proportion of patients who have a partial or complete response to therapy (as best response). As regards PFS and OS, patients without the event were considered as censored at the time of the last follow-up. Patients were assessed with radiological imaging as per clinical practice every 3-4 months and RECIST (version 1.1) criteria were used to define disease progression.

3.2 High-dimensional flow cytometry analysis of patients' PBMCs

PBMCs were first thawed and counted, then 500.000 cells were stained with Live/Dead Fixable Viability Stain 575V for 10 minutes at RT to exclude dead cells from the analysis. After washing, cells were incubated for 10 minutes at RT with 20% human serum to minimize antibody non-specific interaction. Surface staining was then performed using the antibodies listed in Table 1. PBMCs were incubated with antibodies for 15' at room temperature after dead staining. For the unsupervised analysis, data were initially processed in FlowJo (version 10.10.0) for spillover correction and dead cell and

doublet exclusion. For downstream analysis, a random down-sampling was applied: 3.000 $CD45^+$ events for the mieloid panel and 10.000 $CD3^+$ events for the T cell panel, were performed. Processed FCS files were then exported and analyzed in R (version 4.3.1). To minimize technical variability, samples with high signal inconsistency were excluded prior to downstream processing. Data batches were imported using the read.flowSet function from the flowCore package (version 2.14.2). A logical transformation was applied to harmonize marker scales across samples. Batch effects, due to technical rather than biological variations, were corrected and normalized using the gaussNorm function from the flowStats package (version 4.14.1). After normalization, samples were concatenated into a SingleCellExperiment object in R using the prepData function from the CATALYST package (version 1.26.1). Dimensionality reduction was performed with Uniform Manifold Approximation and Projection (UMAP) to visualize cellular relationships in reduced dimensions. High-resolution unsupervised clustering was carried out using FlowSOM (version 2.10.0), followed by metaclustering with ConsensusClusterPlus (version 1.66.0). Clustering was based on marker expression profiles of the $CD45^+$ events.

3.3 Animal studies and reagents

C57BL/6 and transgenic OT-I mice were obtained from Charles River (Calco, Italy) and housed in the pathogen-free animal facility of San Raffaele Scientific Institute. All procedures were performed in accordance with institutional guidelines for animal care and use and in compliance with ARRIVE guidelines. B16F1-gp100 cell line was maintained in IMDM complete medium (10% FBS supplemented with penicillin, streptomycin, glutamine and Hepes). Simvastatin, Geranylgeranylgeranyol (GGOL), Zaragozic Acid A (ZAA), GGTI-2147 and Ovalbumin were from Sigma. The p38 inhibitor SB203580 was purchased from Selleck Chemicals. Carboxyfluoresceinsuccinimidyl ester (CFSE) (Thermofisher) was used at 0.5 μM.

3.4 In vivo experiments

C57BL/6 mice were injected subcutaneously with 2 x10^5 B16F1-gp100 cells. Tumor volume was determined by measuring three perpendicular axes with a caliper every 2 days. Data are reported as the average tumor volume ± sem. We treated mice at day 7 from the inoculum of the tumor with simvastatin 200 μg/mice daily intraperitoneal (i.p.) and at day 9 with anti-PD-1 mAb 200 μg/mice i.p. twice a week. For the two groups in which simvastatin was administered before tumor engraftment, we started the daily treatment 5 days before the inoculum (day-5). The p38 inhibitor SB203580, administered at 200 μg/mice, was given daily i.p. starting at day 7.

3.5 Analysis of tumor-infiltrating immune cells

Tumors were harvested 10 days after injection, minced into small fragments and digested for 20 minutes at 37°C with 66 μg/ml Liberase TL (Roche) and 150 μg/ml DNAse I (Roche). The resulting cell suspension was filtered through a 70 μm cell strainer to obtain single cells. Cells were then stained with Live/Dead fixable near-IR dye (Invitrogen) for 10 minutes at room temperature (RT). After washing, Fc receptors were blocked using 1 μg/100 μl anti-CD16/32 (mouse Fc Block, Biolegend) for 5 minutes at RT. Subsequently, cells were incubated with the antibody cocktail for 15 minutes at RT. Staining was performed using the antibodies listed in Table 1. Samples were acquired by CytoFLEX LX (Beckman Coulter) and analyzed by FlowJo software.

3.6 Generation of bone-marrow derived dendritic cells

Bone marrow cells were isolated from femur and tibia of C57BL/6 mice and then cultured for 6 days in RPMI 1640 complete media (10% FBS with penicillin, streptomycin, glutamine, Hepes and 2-Mercaptoethatol 50 uM) supplemented with 20 ng/mL of IL-4 (Peprotech) and 20 ng/mL of GM-CSF (Peprotech). Differentiation into dendritic cells was confirmed by flow cytometry by a positivity of both CD11c and MHC-II. After 5-6 days of culture BMDCs were treated with the indicated compounds and used for the downstream analyses.

3.7 Antigen presentation assay and intracellular cytokines detection

BMDCs were harvested and plated at a density of $2x10^4$/well in 96 flat-well plate. Splenic OT-I were purified with naive CD8a microbeads (Miltenyi) and labeled with CFSE 0.5 μM and then plated at a density of $2x10^5$/well together with BMDCs and in presence of Ovalbumin 100 μg/ml and IL-2 10 ng/ml in RPMI complete medium. Cells were cultured at 37°C for 3 days and analyzed by flow cytometry for CFSE dilution on $CD8^+$ alive T cells. For cytokines detection BMDCs were treated with simvastatin 10 μM, ZAA 10 μM, simvastatin plus GGOL 40 μM or vehicle overnight. p38 inhibitor SB203580 was added 30 minutes before the other compounds at 10 μM. Treated BMDCs were plated in 24-well plate at concentration of $5x10^5$ and activated with LPS 100 pg/ml for 8 hours. Brefeldin (10 μM) was added 2 hours after LPS addition for 6 hours. Cells were then collected, fixed and permeabilized (eBioscience, Foxp3 Transcription Factor Staining Buffer Set) and analyzed for TNFa and IL-1β by flow cytometry.

3.8 IL-1β secretion assay (ELISA)

BMDCs were harvested and seeded at a density of $5x10^5$/well in 24-well flat-bottom plates. Cells were treated with 10 μM simvastatin or vehicle control for 14-16 hours. Following treatment, the medium was replaced with fresh complete medium, and BMDCs were stimulated with LPS (100 pg/ml). After 24 hours, culture supernatans were collected and analyzed for secreted IL-1β concentration using an ELISA kit (ELISA MAX™ Deluxe Set, Biolegend) according to the manufacturer's instructions.

3.9 Western blot

BMDCs were treated according to the conditions described and lysed in RIPA buffer supplemented with Halt™ Protease and Phosphatase Inhibitor Cocktail (ThermoFisher Scientific). Lysates were centrifuged at 20.000 x g at 4°C. Proteins were measured using BCA Protein Assay Kit (ThermoFisher Scientific) and lysates were prepared with the addition of 4x Laemmli Sample Buffer (BioRad Laboratories) and boiled for 5 min at 95° C. Equal amounts of proteins were loaded in SDS-PAGE and transferred to PVDF membranes. The membranes were blocked with 5% non-fat milk in TBS-T buffer, washed by TBS-T buffer and incubated overnight with primary antibodies against phospho-p38

(Cell Signaling Technology) diluted 1:1000 in 5% BSA in TBS-T buffer. Twelve hours later, membranes were washed and incubated for 1 hour at RT with HRP-conjugated goat anti-rabbit IgG (Southern Biothech) diluted 1:20.000 by 5% non-fat milk in TBS-T buffer. Clarity Western ECL substrate (BioRad Laboratories) was used for protein's detection.

3.10 Intracellular detection of phospho-p38

Cells were treated with simvastatin or vehicle control. After 24 hours, they were harvested and stained for viability and surface markers CD11c and MHC-II. Subsequently, cells were fixed and permeabilized and stained for phospho-p38. Following two washing steps, donkey anti-rabbit IgG conjugated with Alexa Fluor 488 (ThermoFisher Scientific) was added for 15' at RT. After two washing steps, samples were analyzed by flow cytometry.

3.11 Quantitative real-time PCR

BMDCs were treated as previously described for 24 hours. Total RNA was purified using TRI Reagent (Direct-zol RNA Kit, Zymo Research). Reverse transcription was performed by MLV-reverse transcriptase (Promega). Quantitative PCR was performed using SYBR Green Master Mix (Applied Biosystems) on 7900HT Fast Real-Time PCR System (Applied Biosystems). PCR reactions were done in triplicate. The comparative CT method was used to quantify transcripts that were normalized for mouse Actin. The following primers were used: β-Actin forward: 5'-AGA GGG AAA TCG TGC GTG ACA-3', reverse: 5'-CAC TGT GTT GGC ATA GAG GTC-3'; NLRP3 forward: 5'-ATC AAC AGG CGA GAC CTC TG-3', reverse: 5'-GTC CTC CTG GCA TAC CAT AGA-3'; IL1-β forward: 5'-GCA ACT GTT CCT GAA CTC AAC T-3', reverse: 5'-ATC TTT TGG GGT CCG TCA ACT-3'; Interferon-β forward: 5'-ATG AGT GGT GGT TGC AGG C-3', reverse: 5'-TGA CCT TTC AAA TGC AGT AGA TTC-3'; TNF-α forward: 5'-AGG GAT AAG TTC CCA AAT G-3', reverse: 5'-CAC TTG GTG GTT TGC TAC GAC-3'; Caspase-1 forward: 5'-ACA AGG CAC GGG ACC TAT G-3'; reverse: 5'-TCC CAG TCA GTC CTG GAA ATG-3'

3.12 Statistics

The number of animals per group was determined to minimize animal use while ensuring sufficient statistical power to meet the study objectives. Sample size calculations were based on a type I error rate of 5% ($\alpha = 0.05$) and a power equal to 80% ($1-\beta = 0.80$), consistent with the experimental design. Comparisons between two independent groups were performed using Student's t-test, while multiple group comparisons were analyzed by one-way ANOVA. Overall survival was assessed using the log-rank test. All statistical analyses were conducted using GraphPad Prism software.

Table 1. Comprehensive list of anti-human and anti-mouse antibodies used for flow cytometry.

Anti-human antibody	**Clone**	**Company**	**Catalog**
Lymphocyte panel			
CD39 BB515	TU66	BD Horizon	565469
HLA-DR APC-H7	G46-6	BD Pharmigen	561358
CD8 BV605	SK1	BD Horizon	564116
CD45 BUV395	HI30	BD Horizon	563792
CD3 BUV496	SK7	BD OptiBuild	741206
CD45RA BUV737	HI100	BD Horizon	612847
CD95 FAS PE-Cy7	DX2	BD Pharmigen	561633
CD27 BV650	L128	BD Horizon	563228
TIGIT BB700	741182	BD OptiBuild	747846
LAG3 APCR700	T47.530	BD Horizon	565775
ICOS BV421	DX29	BD Horizon	562901
PD1 BV480	EH12.1	BD Horizon	566112
CD137 PE	4B4-1	BD Pharmigen	561701
CD69 BV750	FN50	BD Horizon	568285
CD4 BUV563	SK3	BD Horizon	612913
CD62L BUV615	DREG-56	BD OptiBuild	751546
CD127 BUV805	HIL-7R-M21	BD OptiBuild	748486
TCRgd BV711	11F2	BD Horizon	568490
TIM3 BUV661	7D3	BD Horizon	Custom
CTLA-4 BB660 P2	BNI3	BD Horizon	Custom
CD122 BB790 P	Mik- β3	BD Horizon	Custom
CD25 PE-efluor610	CD25-4E3	Invitrogen	61-0257-42
FOXP3 AF647	259D/C7	BD Pharmigen	560045
Fixable Viability Stain 575V	-	BD Horizon	565694

Anti-human antibody	Clone	Company	Catalog
Myeloid panel			
CD45 BUV496	HI30	BD Horizon	569101
CD14 FITC	M5E2	BD Pharmigen	555397
CD11C APCR700	3.9	BD Horizon	566610
CD56 APC eFLUOR780	TULY56	Invitrogen	47-0566-42
CD11B APC	ICRF44	BD Pharmigen	550019
CD16 BV421	3G8	BD Horizon	562874
HLADR BV480	G46-6	BD Horizon	566113
CD123 PE	7G3	BD Pharmigen	554529
CD20 NovaFB660 120S	2H7	Invitrogen	H076T03B08
CD3 BUV563	UCHT1	BD OptiBuild	748569
CD33 RB780	P67.6	BD Horizon	569096
CD80 BUV395	L307.4	BD Horizon	565210
CD206 BV711	19.2	BD OptiBuild	740797
CD163 PE-Cy7	eBIOGHI/61	Invitrogen	25-1639-42
PD-L1 PE CF594	MIH1	BD Horizon	563742
Fixable Viability Stain 575V	-	BD Horizon	565694

Anti-mouse antibody	Clone	Company	Catalog
CD45 FITC	30-F11	Biolegend	103108
CD45 PerCP	30-F11	BD Pharmigen	557235
CD11B APC-Cy7	M1/70	Biolegend	101226
Ly6c BV510	HK1.4	Biolegend	128033
Ly6g PerCP/Cy5.5	1A8	Biolegend	127616
Ly6g Alexa Fluor 700	1A8	Biolegend	127622
CD11c BUV737	N418	Invitrogen	367-0114-82
F4/80 APC	BM8	Biolegend	123116
MHC-II PE-efluor610	M5/114.15.2	Invitrogen	61-5321-82
PD-L1 PE	MIH5	BD Pharmigen	558091
PD-L1 BUV395	MIH5	BD OptiBuild	745616
CD40 eFluor450	HM40-3	Invitrogen	48-0402-82
CD3 PE	145-2C11	Biolegend	145-2C11
CCR7 BV650	4B12	BD Horizon	564356
Live/dead fixable near IR	-	Invitrogen	L34982

Chapter 4

RESULTS

4.1 Patients with metastatic melanoma on statin therapy have better OS and PFS when treated with checkpoint inhibitor

We performed a retrospective single-center observational study using clinical data derived from the Melanoma Department of Istituto Nazionale Tumori IRCCS Fondazione G. Pascale, Naples, Italy. The study evaluated, in patients with metastatic melanoma, the impact of concomitant statin therapy at the initiation of immunotherapy on clinical outcome assessed as progression free survival (PFS), overall survival (OS) and objective response rate (ORR). As illustrated in Table 2, total number of patients was 66, of which 20 were already receiving statin therapy prior to the initiation of immunotherapy and 46 were not. In accordance with Italian guidelines at the time of database collection patients were treated with single-agent immunotherapy, 52 patients receiving nivolumab and 14 pembrolizumab. Immunotherapy was administered as a first-line therapy for 38 patients and as a second or subsequent line for the other 28 patients. The median age was 65 (range: 21–86), male/female ratio was 42/24. BRAFV600 mutation was present in 26 patients.

Table 2. Clinical characteristics of patients with stage IV melanoma

Clinical Characteristics	**Statin** N = 20	**No Statin** N = 46
Median age (range)	63.5 (21-91)	60.9 (31-81)
Sex (M/F)	12/8	30/16
BRAF WT	12 (60%)	24 (52%)
BRAF V600 Mut	8 (40%)	20 (43%)
AJCC staging • M1a • M1b • M1c • M1d	No. (%) 3 (15%) 6 (30%) 10 (50%) 1 (5%)	No. (%) 2 (4,3%) 7 (15,2%) 33 (71,7%) 4 (8,7%)
Prior treatments • Target Therapy • Immunotherapy • Chemotherapy • TT/Immuno/Chemo • No previous treatment	No. (%) 2 (8.7) 2 (8.7) 1 (4.3) 1 (4.3) 17 (73.9)	No. (%) 3 (6.9) 11 (25.6) 0 (0) 9 (20.9) 20 (46.5)

Best Response	No. (%)	No. (%)
• CR	6 (30)	2 (4.3)
• PR	8 (40)	10 (21.7)
• SD	5 (25)	15 (32.6)
• PD	1 (5)	19 (41.3)

Median-PFS was 52.88 months (95% confidence interval [CI], 32.29 to 62.03) in statin cohort vs. 8.76 months (95% CI, 4.18 to 19.31) in non-statin cohort (p = 0.01). Median-OS was not reached in statin group vs. 29.25 months (95% CI, 18.99 to 43.17) in non-statin group (p = 0.03) (Figure 12). Also, the ORR was strongly significant in favor of statin group: 70% vs. 26.1% (p = 0.002) (Figure 13).

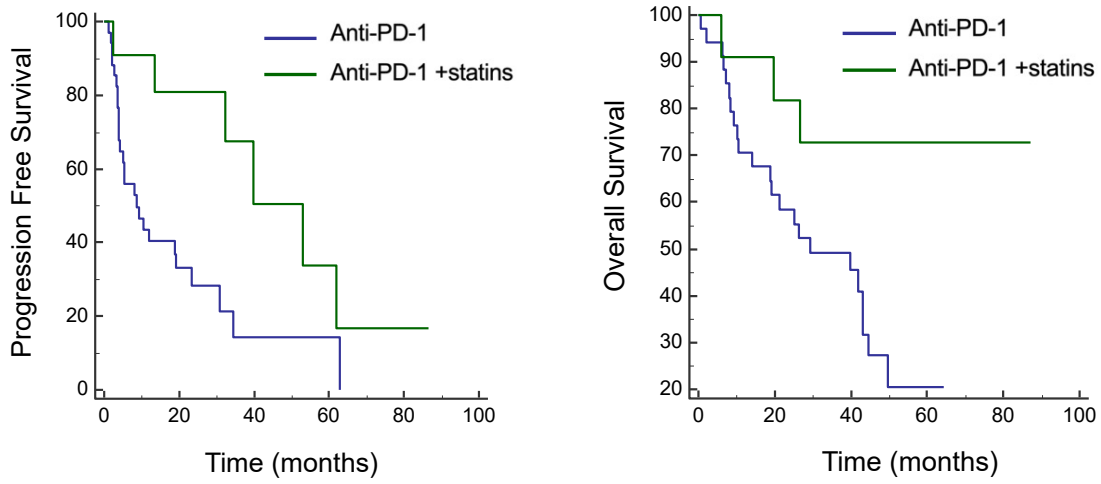

Figure 12. Kaplan-Meier curves showing Progression Free Survival (PFS) (*P* = 0.01) and Overall Survival (OS) (*P* = 0.03) of 66 patients with metastatic melanoma treated with anti-PD-1 antibodies and stratified by use of statins at baseline (Log-rank test).

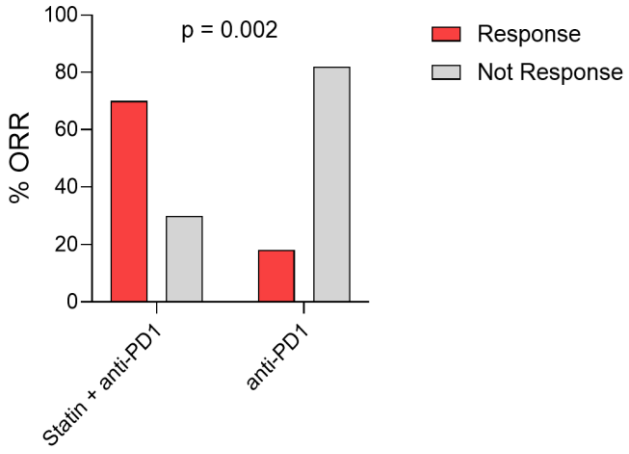

Figure 13. Objective Response Rate to anti-PD1 treatment in statin vs. non statin users. *P* = 0.002 (Fisher's exact test).

To confirm the independent association between statin use and improved PFS and OS was run a multivariate analysis accounting for tumor burden, line of therapy, BRAF mutation status and age. As illustrated in Table 3, the association was confirmed both for PFS and OS (p = 0.039 and 0.028 respectively). We also detected an association between age and PFS (p = 0.026).

Table 3. Multivariate analyses for PFS and OS in statin cohort vs. non-statin cohort

Test variables	HR for PFS (95% CI)	*P* value	HR for OS (95% CI)	*P* value
Statin use Yes versus No	0.29 (0.09-0.94)	**0.039**	0.17 (0.04-0.83)	**0.028**
Age <65 versus ≥ 65	0.37 (0.15-0.89)	**0.026**	1.50 (0.60-3.78)	0.39
BRAFV600 mutation Mutated versus wild-type	0.76 (0.35-1,64)	0.49	0.69 (0.31-1.56)	0.37
Line of therapy First line versus more than one line	0.74 (0,31-1,76)	0.50	1.24 (0.49-3.18)	0.65
Tumor burden M1a-b versus M1c-d cohort	0.83 (0.32-2.18)	0.70	1.27 (0.45-3.58)	0.65

These findings led us to hypothesize that statin use may have enhanced the efficacy of immune checkpoint inhibitors in patients with metastatic melanoma. The underlying mechanisms remain unclear. Given that statins are known to exert immunomodulatory effects on the immune system and considering that numerous studies investigating statins in solid tumors (in the absence of immunotherapy) have yielded inconclusive results, we focused this work on exploring the potential immunological impact of statins. Specifically, we hypothesized that statins may have reprogrammed the tumor microenvironment, rendering it more responsive to immunotherapy. To investigate this hypothesis, we first analyzed peripheral blood mononuclear cells (PBMCs) from our cohort of patients affected by melanoma and subsequently evaluated the efficacy of the combination of statins plus anti-PD1 therapy in the B16 melanoma model.

4.2 PBMC analyses of patients with metastatic melanoma on statin therapy reveal a peripheral increase in terms of APCs

Biological studies, particularly those analyzing circulating immune cell profiles in statin users undergoing immunotherapy, remain scarce. In this study, we employed high-dimensional (HD) flow cytometry to analyze 21 PBMC samples from our cohort of 66 patients with metastatic melanoma (Table 2), to identify immune cell subsets potentially associated with differential clinical outcomes. PBMCs were collected prior to initiation of immunotherapy (T0): 12 samples from non-statin users and 9 from statin users. Two flow-cytometry panels were designed to characterize myeloid and lymphoid compartments (Table 1). Of the 21 PBMCs analyzed, 14 (7 statin users and 7 non-users) were evaluable for the myeloid panel, and 16 (8 statin users and 8 non-users) for the lymphoid panel. Additionally, longitudinal samples were available from statin users 6 months post-immunotherapy initiation, comprising 5 samples evaluable for the myeloid panel and 7 for the lymphoid panel. Unsupervised clustering of myeloid cells at T0 identified 10 clusters with differential representation between the two groups (Figure 14, a-c). Statin users exhibited significant increases in antigen-presenting cell (APC) subsets (Figure 14, c): inflammatory/activated monocytes ($CD11c^{+}CD14^{+}HLA\text{-}DR^{+}$), which further increased 6 months after the onset of immunotherapy (Figure 15, c), plasmacytoid dendritic cells ($CD11c^{-}CD123^{high}HLA\text{-}DR^{+}$), and a $CD11c^{+}CD123^{low}CD33^{+}$ cell population (Figure 14, c). Further analyses on the $CD11c^{+}CD14^{+}HLA\text{-}DR^{+}$ monocyte-derived cells, using anti-CD14, -CD16, -CD33, -CD11b, -CD11c, -CD88/89, -CD163 and HLA-DR monoclonal antibodies (mAbs), allowed to distinguish between activated monocytes and the recently described DC3 cells[142,143]. Indeed, < 5% of the cells were DC3, with > 95% being activated monocytes (Figure 16). Collectively, the APC subsets were significantly enriched in PBMCs from statin users (6% vs. 2%, $p = 0.012$; Figure 17). Interestingly, PD-L1 expression in APCs was significantly reduced in statin users (27.2% vs. 11.6%, $p = 0.016$), suggesting a lower immunosuppressive potential of this cell population (Figure 17)[144].

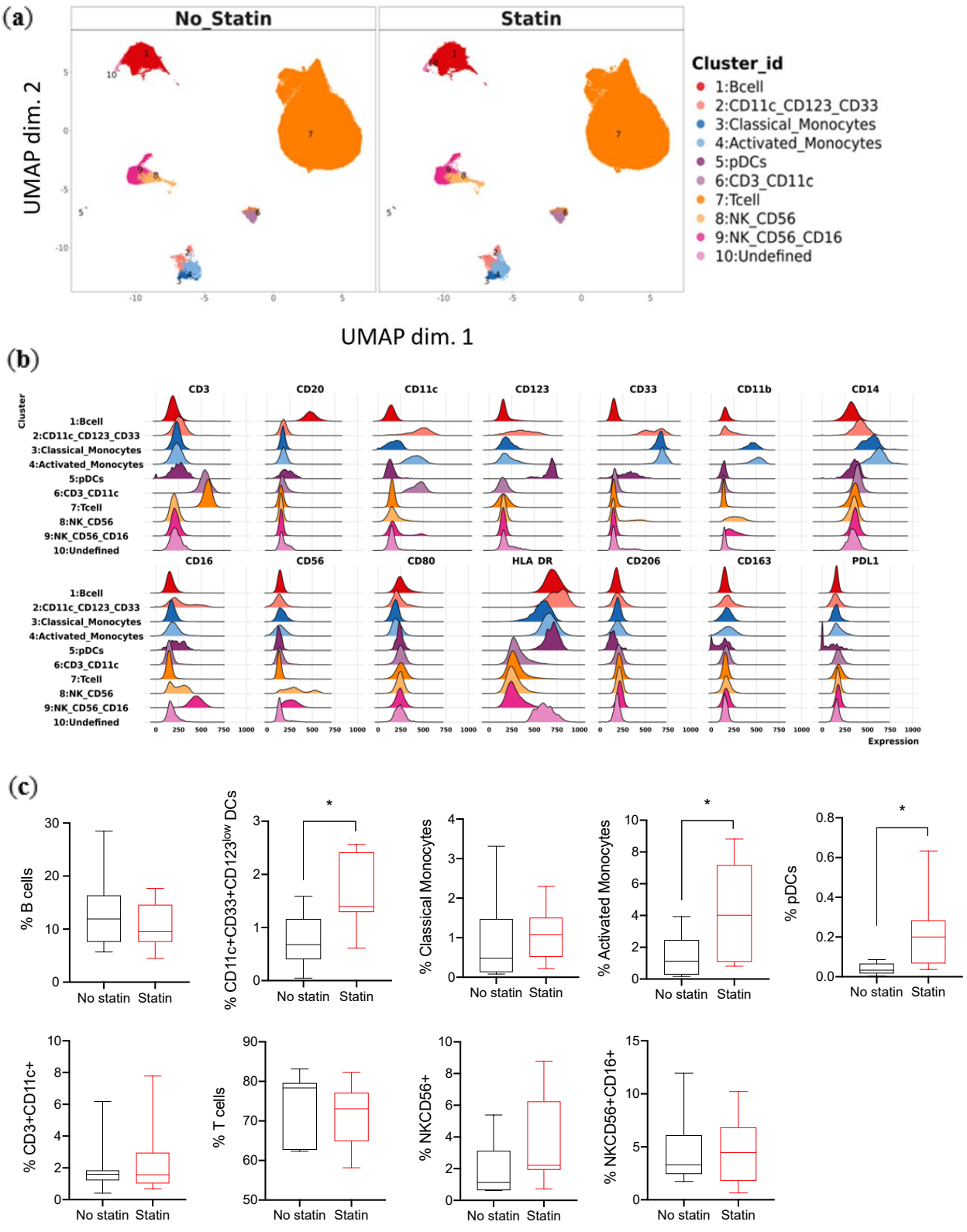

Figure 14. Uniform manifold approximation and projection (UMAP) (**a**), fluorescence intensity for each marker (**b**) and box plots (**c**) of the different clusters of myeloid subsets identified in 8 non-statin and 8 statin patients before the onset of immunotherapy (T0). **P* < 0.05 (Mann-Whitney test).

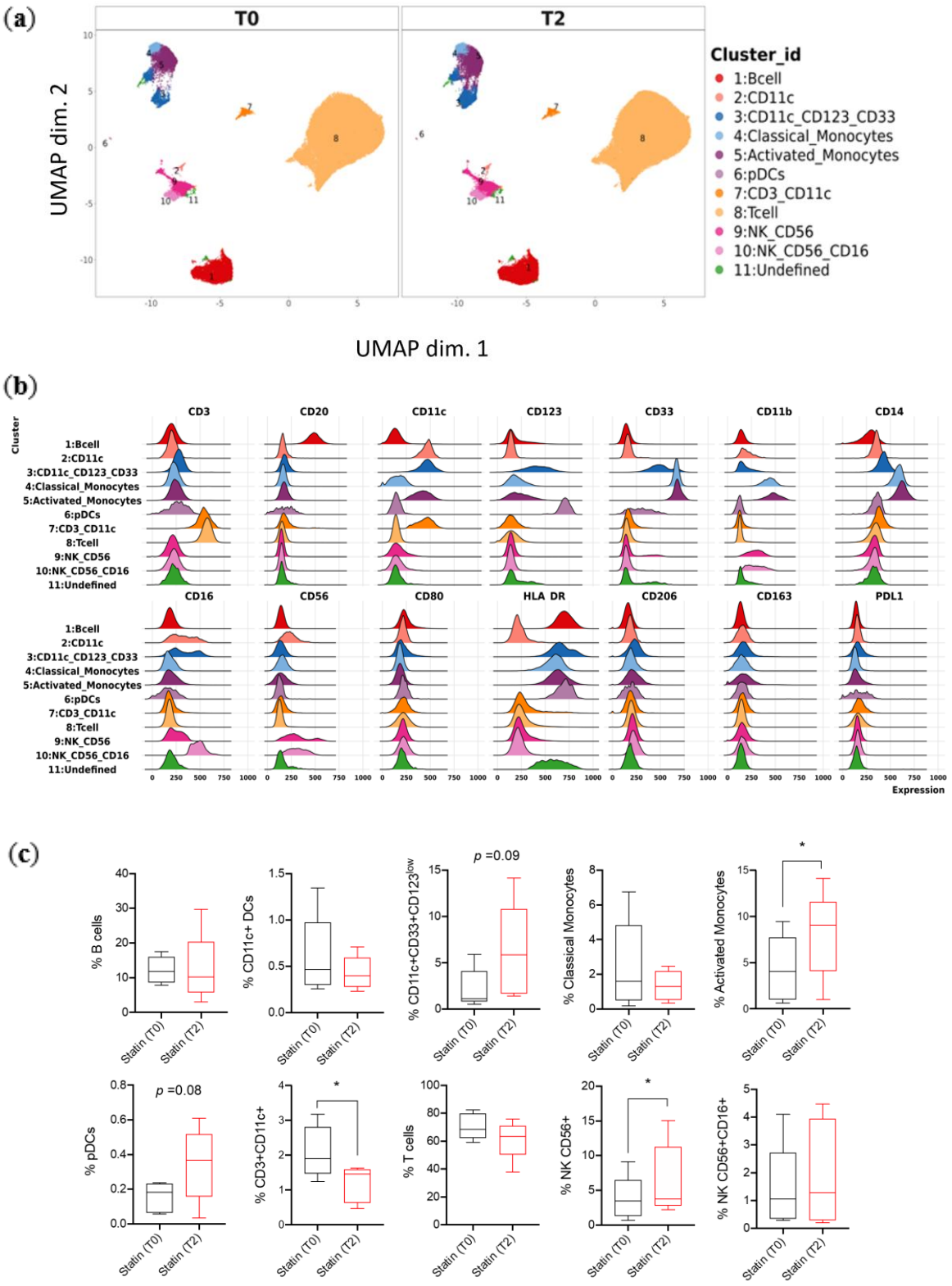

Figure 15. Uniform manifold approximation and projection (UMAP) (**a**), fluorescence intensity for each marker (**b**) and box plots (**c**) of the different clusters of myeloid subsets identified in 7 non-statin and 7 statin patients before and 6 months after the onset of immunotherapy (T0 vs. T2). **P* < 0.05 (paired t test).

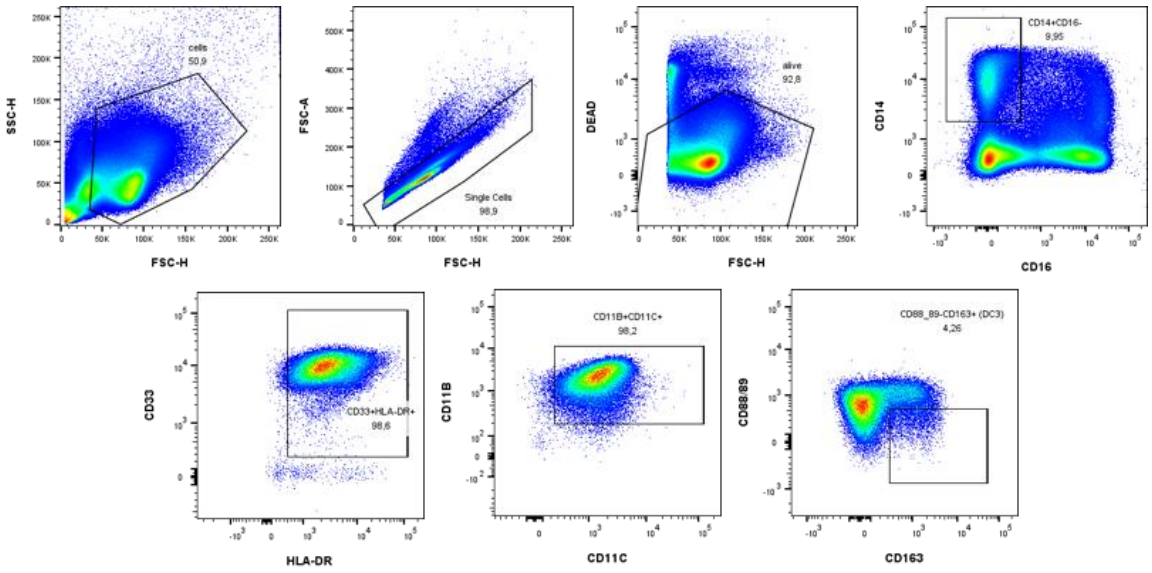

Figure 16. Gating strategy used to identify dendritic cells type 3 subpopulation by flow cytometry.

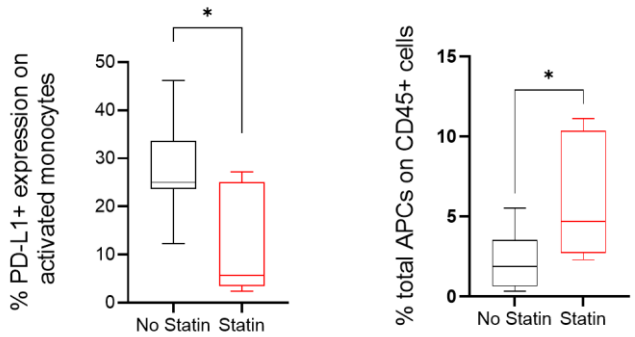

Figure 17. Box plot analysis showing the percentage of PD-L1 expression on activated monocyte and the percentage of total APC subsets on CD45+ cells before the onset of immunotherapy (T0). *$P < 0.05$ (unpaired t-test).

Next, to detect possible differences of lymphoid subsets between statin and non-statin patients, we performed HD-flow cytometry experiments using the lymphoid panel (Table 1). Unsupervised clustering of lymphoid cells at baseline (T0) identified 20 distinct clusters, with differences in cluster distributions between statin and non-statin users (Figure 18, a-c). Statin users exhibited a significant increase in a population of unconventional $CD3^{+}CD4^{-}CD8^{-}$ T cells expressing CD127, CD95, and PD-1. Conversely, a subset of $CD3^{+}CD4^{+}$ T cells expressing exhaustion markers (ICOS, PD-1, CTLA-4, and TIGIT)[145,146] decreased in statin users (Figure 18, c). At 6 months, PBMCs

from statin users showed the increase of unconventional $CD3^+$ TEMRA cells and a subset of $CD3^+CD4^+$ TEM cells expressing ICOS, previously associated with positive clinical outcomes in patients diagnosed with melanoma treated with anti-CTLA-4 mAbs[147] (Figure 19, c). Nevertheless, although we detected some shifts in lymphoid subset distributions, the demonstration of a reactivation of specific antitumor immunity would require clearer evidence of T-cell modulation, potentially revealed by functional assays given the minimal percentage differences observed. Owing to the limited number of PBMCs, we were unable to include more comprehensive intracellular panels or perform restimulation assays to assess key effector markers such as Granzyme B and IFN-γ. These analyses will be required in future studies to better delineate the impact of statins on T-cell–mediated immunity in patients receiving immunotherapy. Another limitation of this PBMC analysis is the small number of available samples (n = 21), which, despite being randomly selected from the two patient cohorts, may introduce potential sources of confounding. Statin users and non-users might have differed in other clinical variables such as concomitant medications, comorbidities, age, or previous treatments that were not fully controlled for in this exploratory dataset and may have contributed to the observed immune profiles. Although selection was random and no obvious clinical imbalances emerged, the sample size did not allow formal multivariable adjustment. Therefore, these findings should be considered exploratory and hypothesis-generating.

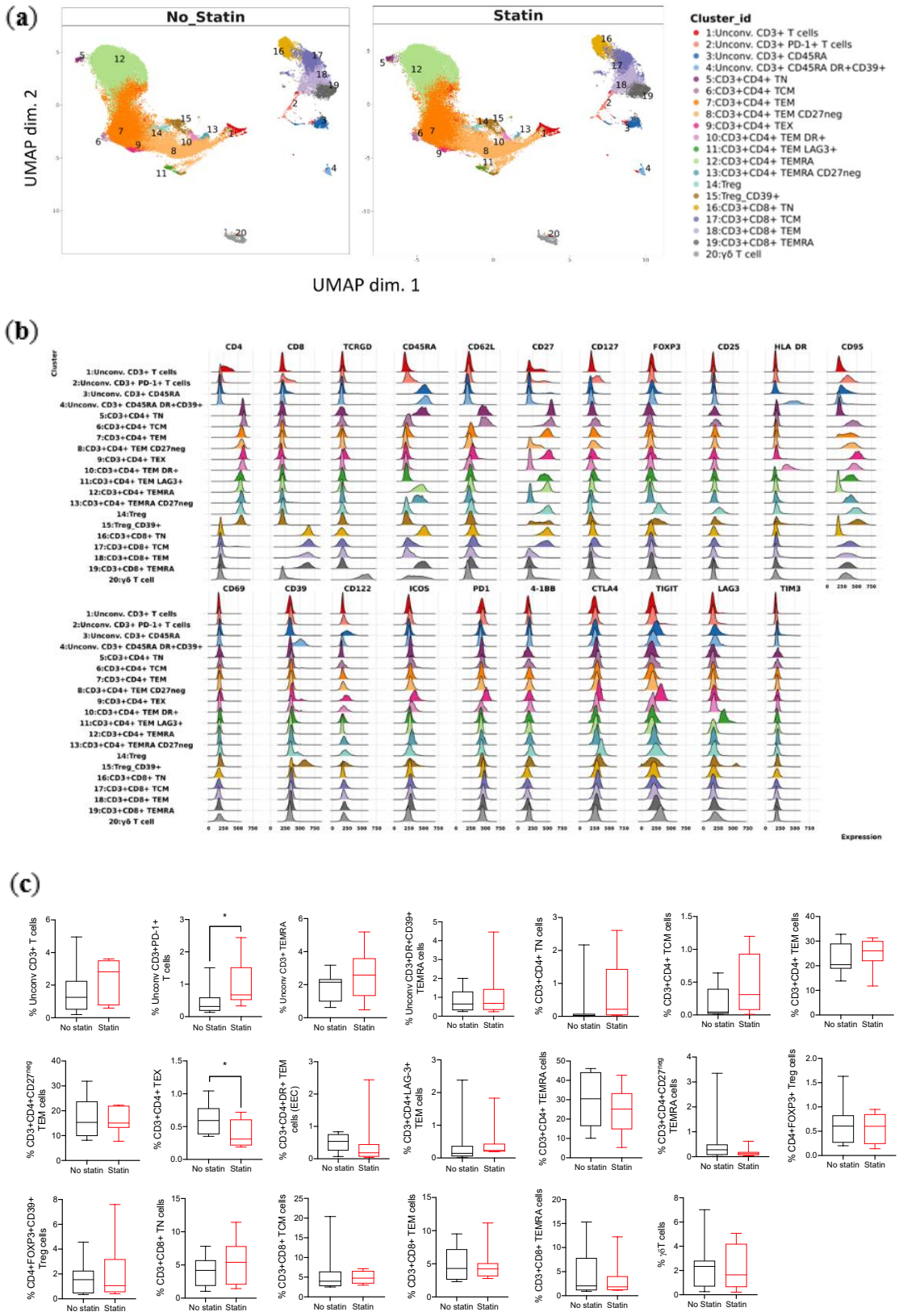

Figure 18. Uniform manifold approximation and projection (UMAP) (**a**), fluorescence intensity for each marker (**b**) and box plots (**c**) of the different clusters of lymphoid subsets identified before the onset of immunotherapy (T0). *$P < 0.05$ (Mann-Whitney test).

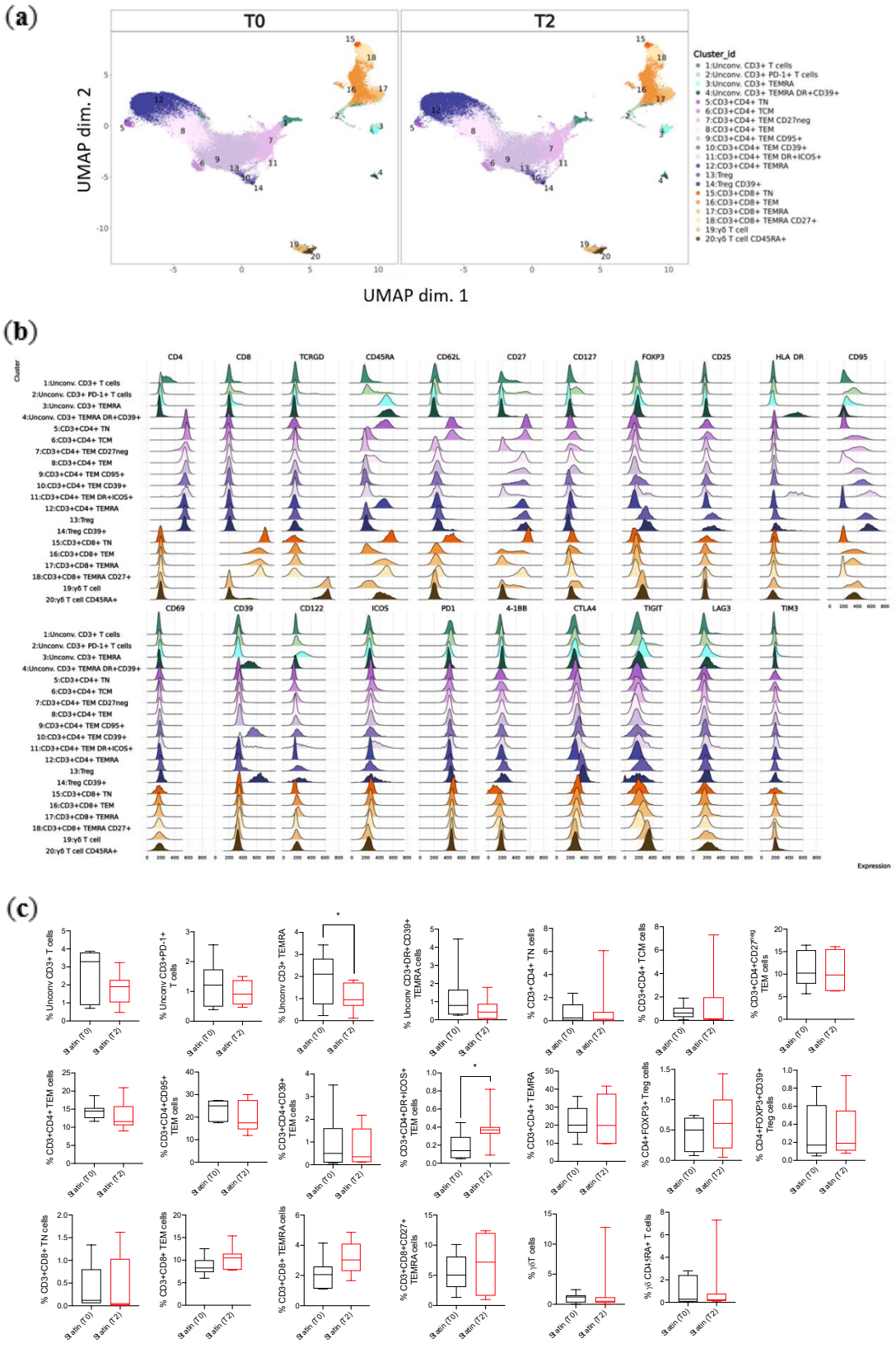

Figure 19. Uniform manifold approximation and projection (UMAP) (**a**), fluorescence intensity for each marker (**b**) and box plots (**c**) of the different clusters of lymphoid subsets identified before and 6 months after the onset of immunotherapy (T0 vs. T2). **P* < 0.05 (paired t test).

4.3 Simvastatin administration before tumor challenge improves the efficacy of anti-PD1 in melanoma-bearing mice

We designed in-vivo experiments to better investigate the effects of statins on immune system observed in patients with melanoma. We treated mice daily with simvastatin starting 5 days before the inoculum of B16-gp100 melanoma cells. At day 8, after tumor establishment, we started administering anti-PD1 mAbs. This schedule was designed to better mimic the clinical context in which patients are already receiving statin therapy prior to cancer onset. This combinatorial regimen significantly improved tumor growth control and extended survival (Figure 20), while simvastatin treatment alone did not. As already described, also anti-PD1 monotherapy was ineffective, consistent with the low immunogenicity of B16 murine model[148]. This lack of efficacy of simvastatin monotherapy is in line with recent evidence showing that tumor-bearing mice display elevated circulating cholesterol together with a reduction in hepatic cholesterol biosynthesis, as reflected by decreased levels of key intermediates such as mevalonate and squalene. This metabolic profile is driven by increased hepatic expression of PCSK9 in response to tumor-associated elevations of IL-1β and IL-6[149]. Such tumor-induced metabolic rewiring may limit the ability of statin to exert antitumor activity when used as single agent, as the lipid-biosynthetic flux on which this drug typically acts is already depressed in the tumor-bearing host.

To determine whether statin modulates APCs function in this model, we performed flow-cytometry analysis of tumor-infiltrating immune cells. Simvastatin treatment induced a significant increase in the percentage of CD40 and in the expression of MHC-II on tumor-infiltrating DCs (Figure 21). The increase was both on DCs type 1 (Lyn- CD11c+ CD11b- Ly6c- MHC-II+) and DCs type 2 (Lyn- CD11c+ CD11b+ Ly6c- MHC-II+).

Taken together, the information from human melanoma PBMCs and B16-gp100 melanoma mouse model led us to hypothesize that statin therapy could synergize with anti-PD1 through a mechanism involving DCs activation.

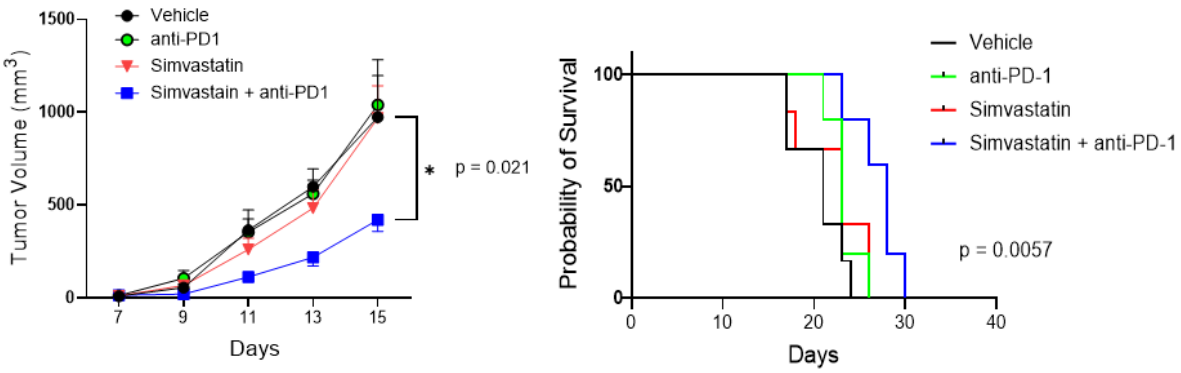

Figure 20. (**a**) B16F1-gp100 growth control in mice pre-treated with simvastatin and then with anti-PD-1 mAb. One experiment out of two is shown (Mean ± s.e.m. n = 4-6 mice/group). P = 0.021 (2way ANOVA). (**b**) Kaplan-Meier analysis of mice bearing B16F1 melanoma and treated as in **a**. One experiment with n = 5-6 mice/group is shown. P = 0.0057 (log-rank test).

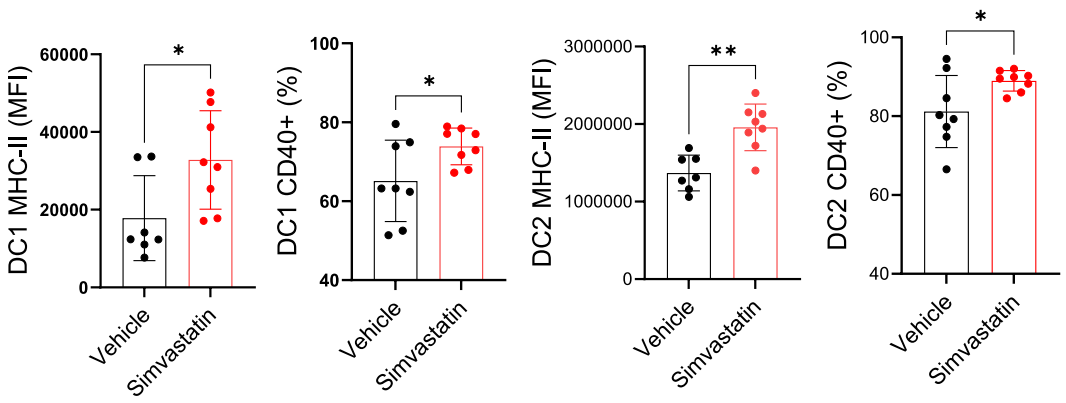

Figure 21. Flow cytometry analysis for the expression of MHC-II and CD40 markers by intratumor DC1 and DC2 collected from vehicle or simvastatin pretreated B16F1-bearing mice. Mean and s.d. of one experiment with 7-8 mice/group. *P < 0.05; **P < 0.01 (unpaired t-test). MFI, Mean Fluorescence Intensity.

4.4 Simvastatin increases the expression of activation markers and proinflammatory genes in mouse bone marrow derived DCs (BMDCs)

To better dissect if simvastatin modulates DCs function, we differentiated mouse bone marrow precursors in-vitro with IL-4 20 ng/ml and GM-CSF 20 ng/ml for 6 days. Then, we treated them with simvastatin 10 μM for 24 hours. As already observed in vivo, we detected an increase in the percentage of CD40+MHC-II+ BMDCs consistent with a phenotype of activated DCs (Figure 22, a). Noteworthy, when supplemented with

ovalbumin, simvastatin-treated BMDCs could prime antigen-specific OT-I T cells more effectively than BMDCs treated with vehicle (Figure 22, b-c), indicating that the observed change of the phenotype results in enhanced BMDCs functionality.

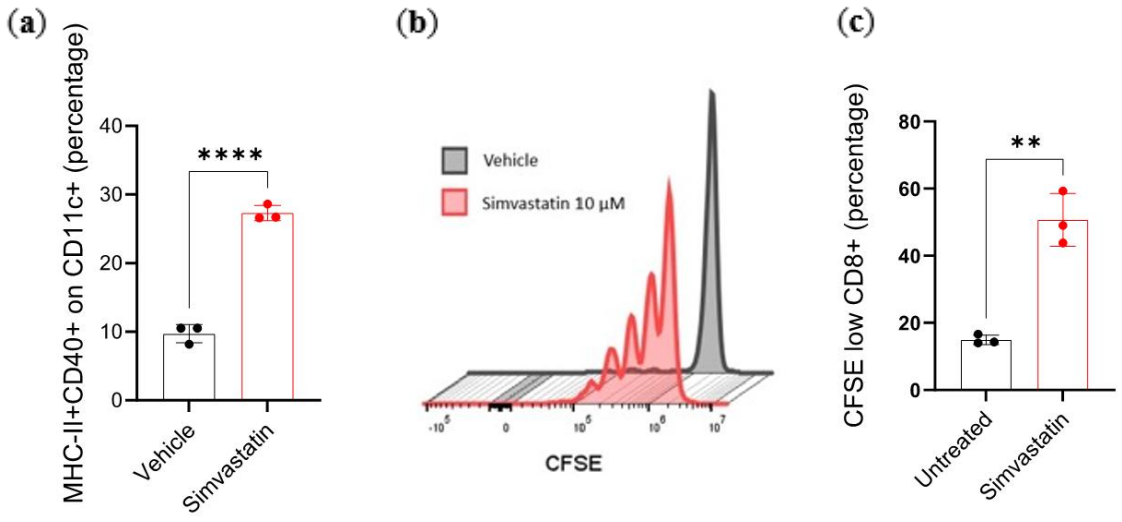

Figure 22. (**a**) Percentage of MHC-II+CD40+ activated DCs among the CD11c+ cells. *$P < 0.05$ (unpaired t-test). (**b**, **c**) Histograms of CFSE dilution (**b**) and quantification (**c**) of OT-I CD8+ T cells stimulated with BMDCs pretreated with ovalbumin and simvastatin or vehicle. *$P < 0.05$ (unpaired t-test).

Since activated DCs start producing pro-inflammatory cytokines, which in turn play a critical role in restoring the antitumor response following anti-PD1 immunotherapy we asked whether simvastatin might promote the production of pro-inflammatory cytokines. We examined by qPCR the mRNA transcripts of well-described pro-inflammatory genes in simvastatin-treated BMDCs, revealing that simvastatin alone drives the increase of Nlrp3, Caspase1, Il1β, Tnfα and Ifnβ transcripts (Figure 23). As previously reported[110], simvastatin alone was not able to increase the production of IL1β and TNFα cytokines (Figure 24, a), which was indeed observed when BMDCs pretreated with simvastatin, were also treated with LPS. Indeed, BMDCs pretreated with simvastatin and then treated with LPS produced higher levels of IL1β and TNFα cytokines, as compared to control (Figure 24, b). This observation was corroborated by the quantification of secreted IL-1β in the supernatant of BMDCs (Figure 25) and establishes a model of activation in which simvastatin induces the expression of pro-inflammatory genes in DCs, which in the presence of a subsequent and canonical activating stimulus, respond more intensively.

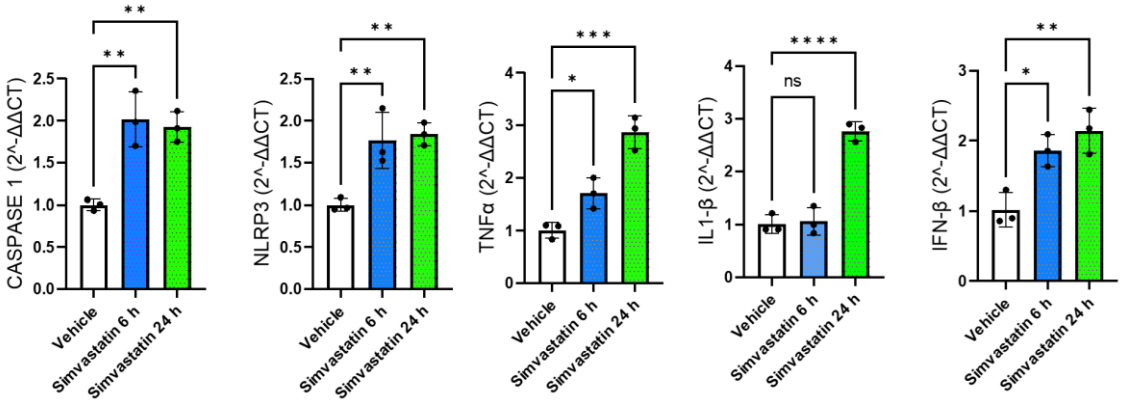

Figure 23. qPCR analysis of the expression of the indicated genes in BMDCs treated with vehicle or simvastatin for 6 and 24 hours. *$P < 0.05$ (unpaired t-test).

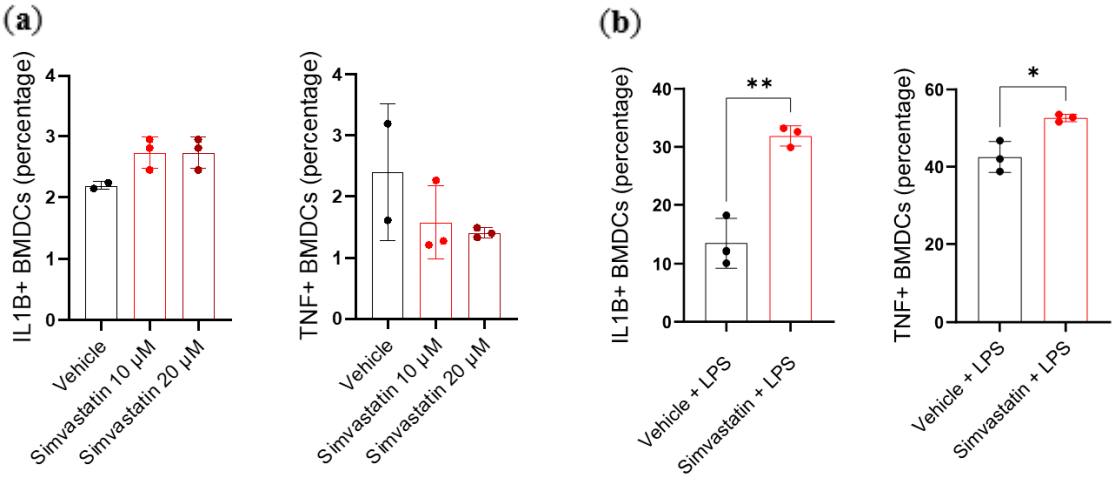

Figure 24. (**a**, **b**) Intracellular flow cytometry analysis of IL-1β and TNF-α expression in BMDCs treated with simvastatin or vehicle (**a**) or treated with simvastatin and vehicle and then stimulated with LPS for 8 hours (**b**). *$P < 0.05$ (unpaired t-test).

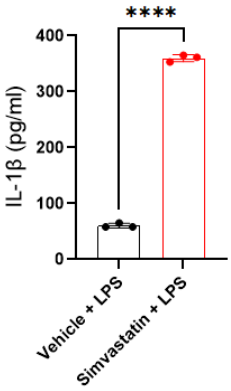

Figure 25. ELISA of IL-1β in the supernatant of BMDCs treated with simvastatin or vehicle and then stimulated with LPS for 24 hours. *$P < 0.05$ (unpaired t-test).

4.5 Simvastatin-mediated activation of BMDCs is driven by isoprenoids synthesis and p38 MAPK phosphorylation

Beyond their well-established role in inhibiting cholesterol biosynthesis, statins also interfere with the production of isoprenoid intermediates, particularly geranylgeranyl diphosphate (GGPP), which is critical for the isoprenylation and membrane localization of small GTPases[70]. Notably, the inhibition of HMG-CoA reductase has been shown to enhance antigen presentation in murine BMDCs by depleting intracellular GGPP, thereby impairing Rab5 lipidation[113]. Moreover, in murine macrophages, statin treatment has been reported to potentiate LPS-induced phosphorylation of p38 MAPK, thereby promoting the production of pro-inflammatory cytokines such as IL-1β[150–152].

To investigate these pathways, we first analyzed p38 MAPK activation in BMDCs using western blotting and flow cytometry and observed enhanced p38 MAPK phosphorylation upon simvastatin treatment (Figure 26, a-b).

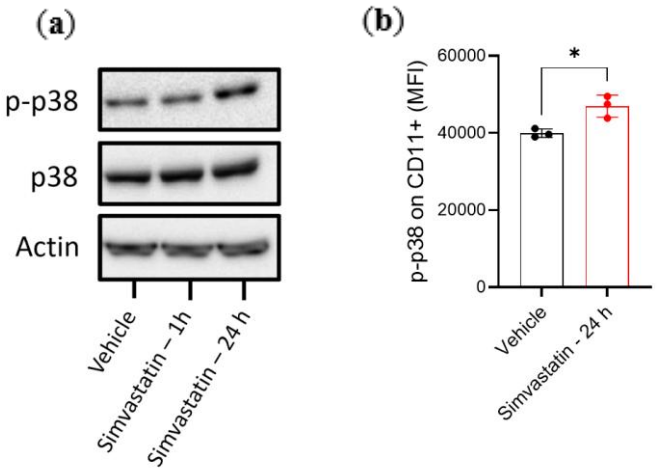

Figure 26. (**a**, **b**) Western blot (**a**) and flow cytometry analyses (**b**) showing intracellular phospho-p38 MAPK in BMDCs treated with vehicle or simvastatin at indicated time. One representative experiment is shown. Mean and s.d. *$P < 0.05$ (unpaired t-test).

To further assess the role of p38 MAPK in DCs activation, and to dissect which branch of the mevalonate pathway could be responsible for the observed effect, we treated BMDCs with simvastatin in the presence or absence of the p38 inhibitor SB203580. Moreover, to evaluate whether cholesterol itself or the blockade of GGPP, were responsible for DCs activation, we employed zaragozic acid A (ZAA), a selective inhibitor of cholesterol synthesis downstream mevalonate, geranylgeraniol (GGOL),

which restores protein geranylgeranylation in presence of simvastatin or the geranylgeranyl transferase inhibitor GGTI-2147, which inhibits protein isoprenylation (Figure 27). Simvastatin-induced upregulation of MHC-II and CD40 was completely abrogated by SB203580 pre-treatment (Figure 28, a-b). Similarly, transcription of pro-inflammatory genes (Figure 29) and LPS-induced intracellular level of IL-1β and TNFα (Figure 30) were also inhibited, underscoring the central role played by p38 MAPK in statin-mediated activation of BMDCs. Importantly, co-treatment with GGOL reversed the simvastatin-induced upregulation of MHC-II and CD40 as well as pro-inflammatory genes transcription and intracellular cytokines levels. In contrast, ZAA, which inhibits cholesterol synthesis downstream of isoprenoid production at the level of squalene, had no effect (Figure 28-30), indicating that statin-induced activation of APCs is mediated by isoprenoid depletion rather than cholesterol reduction.

Finally, to evaluate the in vivo relevance of p38 MAPK signaling, B16F1-gp100 tumor-bearing mice were treated with simvastatin prior to tumor inoculation and subsequently received anti-PD1 mAbs, either alone or in combination with SB203580. An additional group received SB203580 and anti-PD1 mAbs without simvastatin. Again, the combination of simvastatin and anti-PD1 mAbs controlled tumor growth, whereas the addition of SB203580 to simvastatin plus anti-PD1 regimen partially reversed this effect (Figure 31), confirming the pivotal role played by p38 MAPK signaling in mediating the anti-tumor efficacy of simvastatin in our in vivo model.

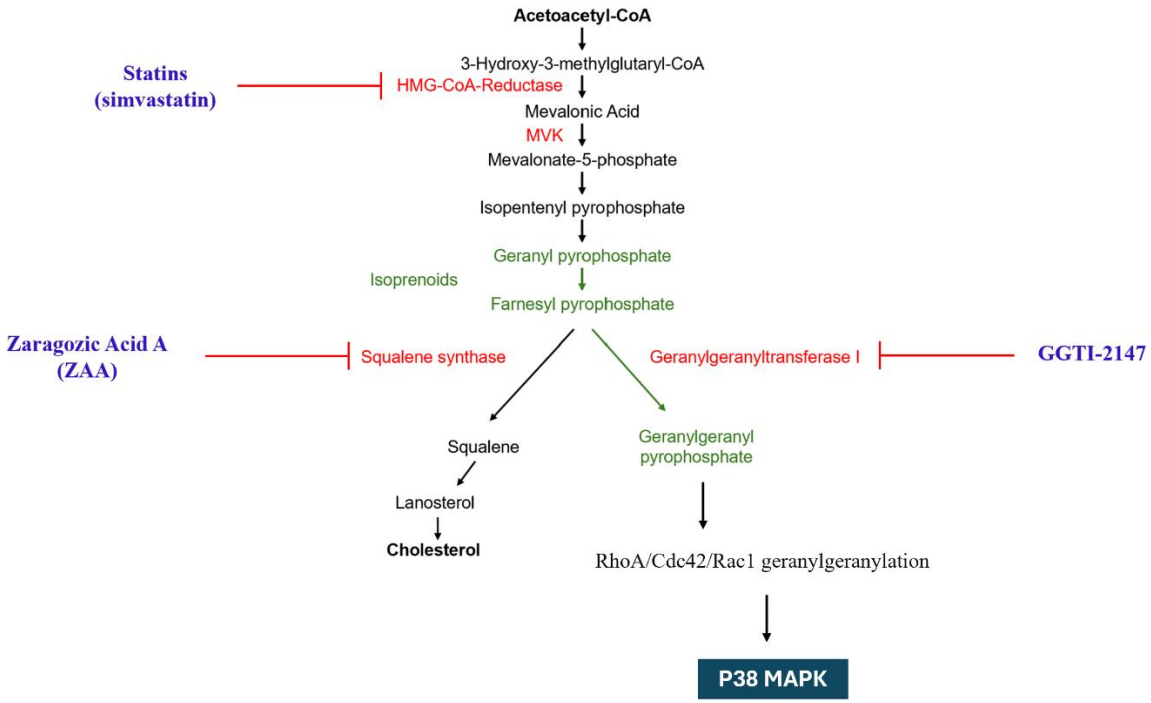

Figure 27. Schematic representation of the mevalonate pathway reporting enzymes inhibited by specific drugs. In green is represented the pathway leading to isoprenoid formation. Statins, *i.e.*, simvastatin inhibits the hydroxymethyglutaryl CoA reductase (HMG-CoA reductase); zaragozic acid A (ZAA) inhibits squalene synthase; GGTI-2147 inhibits protein isoprenylation.

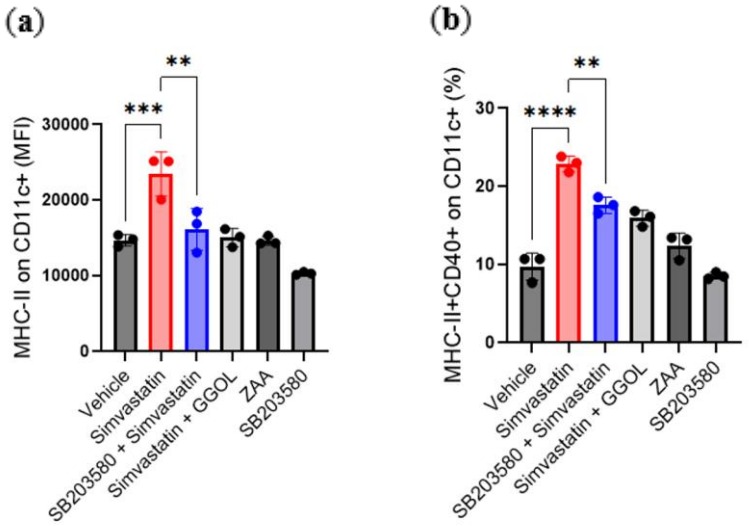

Figure 28. (**a**, **b**) Flow cytometry analysis of MHC-II expression (**a**) and MHC-II and CD40 expression (**b**) on CD11c^{+} BMDCs treated as indicated. Mean and s.d. of 3 independent experiments. $^{**}P < 0.01$; $^{***}P < 0.001$ (unpaired t-test).

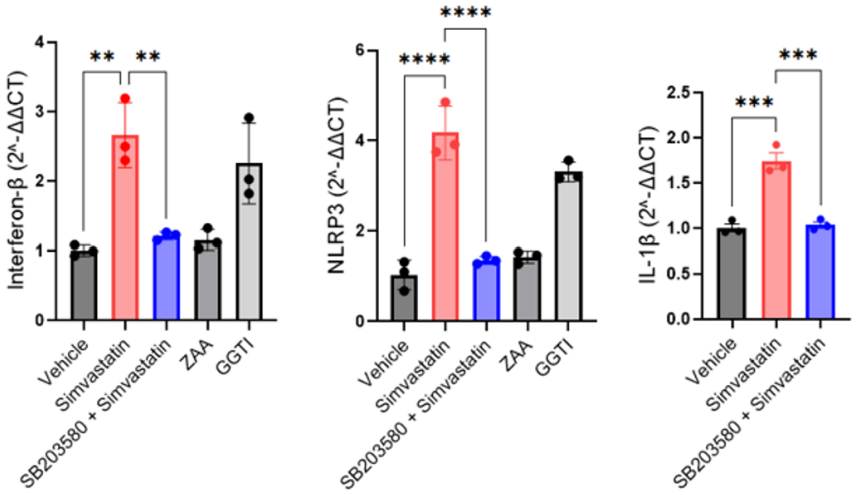

Figure 29. qPCR analysis of *Ifnb*, *Nlrp3* and *Il1b* transcripts in BMDCs treated as indicated. Mean and s.d. of 2 independent experiments. $^{**}P < 0.01$; $^{***}P < 0.001$; $^{****}P < 0.0001$ (unpaired t-test).

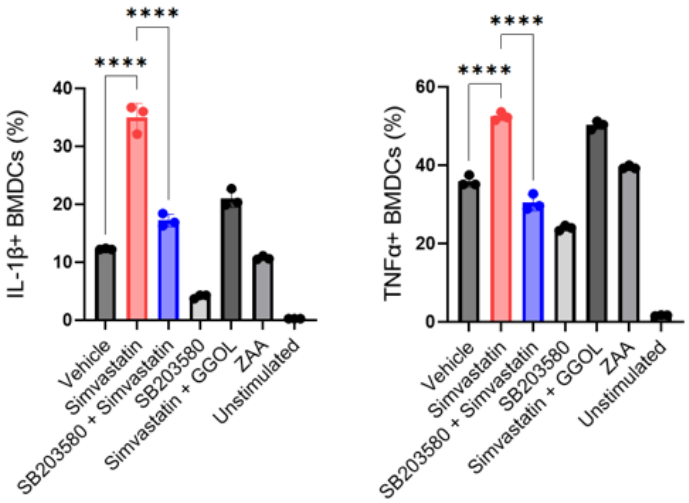

Figure 30. Intracellular flow cytometry analysis of IL1-β and TNF-α expression in BMDCs stimulated with LPS (100 pg) or unstimulated and treated as reported. Mean and s.d. of one experiment. $^{****}P < 0.0001$ (unpaired t-test).

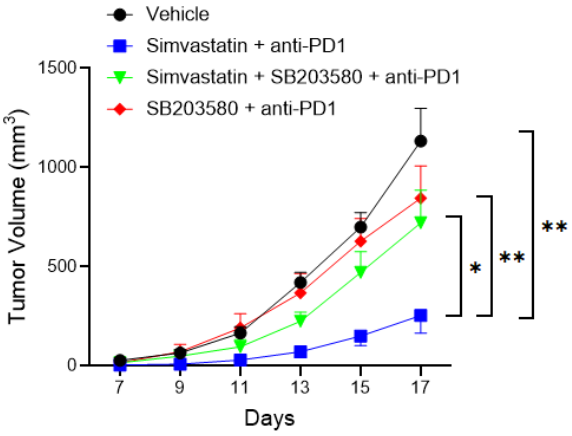

Figure 31. B16F1-gp100 tumor growth control in mice pre-treated with vehicle, simvastatin and subsequently treated with anti-PD-1 mAb alone or with the p38 inhibitor SB203580. (Mean ± s.e.m. n = 4-6 mice/group). *$P < 0.05$; **$P < 0.01$ (2way ANOVA).

Chapter 5

DISCUSSION

The potential role of statins in improving survival in solid tumors has been debated for decades. Since their approval in the late 1980s for the prevention of cardiovascular diseases, numerous studies have investigated whether statin use could reduce the incidence or recurrence of solid tumors[120,121,126,153], without reaching definitive conclusions. However, the advent of immunotherapy has reopened this question, offering a new biological context in which statin therapy should be evaluated[135]. Recent retrospective analyses have reported that statin use, often prescribed for cardiovascular indications, improves the clinical outcome of cancer patients treated with immune checkpoint inhibitors (ICIs)[138–140]. Our study extends these observations by showing an increased frequency of circulating immune cells with antigen presenting abilities, particularly activated monocytes, in patients receiving statins and experiencing significantly better outcomes with immunotherapy in terms of PFS, OS and ORR. This finding is validated by multivariate analysis accounting for tumor burden, line of therapy, BRAF mutation status and age.

Unlike previous reports, we reproduced these data in a preclinical in vivo model, showing that melanoma-bearing mice pre-treated with simvastatin and subsequently treated with anti-PD1 antibodies exhibited reduced tumor growth and prolonged survival, providing experimental support for the clinical findings. The fact that statin therapy was effective when initiated before, but not after melanoma challenge suggests that HMG-CoA reductase inhibitors confer immune cells immunostimulatory properties capable of sustaining the antitumor immune response promoted by anti-PD1 immunotherapy. This hypothesis was confirmed by high dimensional flow cytometry of PBMCs from patients with melanoma, as well as by flow cytometry analysis of tumor-infiltrating immune cells from simvastatin-treated melanoma-bearing mice. Both analyses demonstrated a proinflammatory shift within the APC compartment, with increased frequency of circulating APCs, particularly $CD11c^+$ activated monocytes, and upregulation of CD40 and MHC-II molecules on both DC1 and DC2 within the tumor microenvironment (TME).

The immunomodulatory effects of statins have long been recognized, but whether they derive from the inhibition of cholesterol synthesis, blockade of isoprenoid production, or both, remains debated. Cholesterol itself exerts important regulatory functions on immune cells: its accumulation in $CD8^+$ T cells promotes the induction of an exhaustion

program[114], while its metabolites can inhibit the terminal differentiation of tumor-infiltrating DCs[154]. Conversely, cholesterol depletion in macrophages can elicit proinflammatory responses through the activation of the SCAP-SREBP2 complex and the NLRP3 inflammasome[117]. Beyond their well-known effect on cholesterol synthesis, statins reduce the production of isoprenoids, including geranylgeranyl diphosphate (GGPP). These metabolites are essential for the isoprenylation of small GTPases and therefore for their membrane localization and function. Notably, inhibition of HMG-CoA reductase enhances antigen presentation by murine BMDCs through GGPP depletion, leading to impaired lipidation of the GTPase Rab5[113]. Similarly, GGPP deficiency in macrophages has been shown to activate Rac1, contributing to erosive arthritis in mice[110], and to inhibit RhoA, resulting in pyrin inflammasome activation[111]. Supporting this notion, the autosomal recessive IL-1β-mediated autoinflammatory disorder mevalonate kinase deficiency (MKD) exemplifies how disruption of the mevalonate pathway can trigger aberrant inflammasome activation and proinflammatory manifestations[155].

Although we cannot completely exclude the possibility that the observed increase in $CD11c^+$ monocytes was influenced by hypercholesterolemia[156], particularly given the retrospective nature of our study and recent evidence that elevated cholesterol promotes RORγ-dependent expansion of immunosuppressive monocytic cells[149], this explanation appears unlikely, as patients receiving statins generally maintain well-controlled cholesterol levels. Moreover, the in vivo experiments were conducted in wild-type mice with normal lipid profiles (data not shown). Therefore, using BMDCs as an in vitro model of APCs, we propose that statin therapy promotes a proinflammatory microenvironment through direct effects on immune cells, rather than as a secondary consequence of altered cholesterol metabolism. Specifically, simvastatin promoted DCs activation, as evidenced by the upregulation of costimulatory molecules, increased expression of inflammatory cytokine transcripts, and enhanced antigen-specific $CD8^+$ T-cell proliferation.

Distinct from previous reports[110,150], our study provides, to our knowledge, the first evidence that statin treatment alone can induce p38 MAPK activation even in the absence of LPS stimulation, although, as expected, LPS triggers a much stronger response. Unlike a rapid canonical signaling cascade, p38 MAPK activation occurred with a delay, consistent with the time required for isoprenoid depletion to occur. Supplementation of simvastatin-treated cells with GGOL, or selective inhibition of specific branches of the

mevalonate pathway using ZAA and GGTI, revealed that the inflammatory effect of statins depends on impaired protein isoprenylation. The finding that isoprenoid depletion, normally required for small GTPase activation, results in DCs activation may appear paradoxical. However, as elegantly discussed by Mark R. Philips[157], if Rho GTPase-activating proteins (RhoGAPs) are more dependent on geranylgeranylation than guanine nucleotide exchange factors (GEFs)[158], impaired prenylation may preferentially suppress RhoGAP activity, leading to constitutive Rho GTPase activation and downstream induction of proinflammatory pathways.

In line with previous studies[110,150,159], statin treatment alone did not increase IL-1β or TNFα secretion. However, upon LPS stimulation, cytokine release was markedly amplified compared with vehicle-treated controls. These results indicate that statins can "prime" DCs by inducing both transcriptional changes (*i.e.*, pro-inflammatory cytokines transcripts) and phenotypic remodeling (*i.e.*, increased expression of costimulatory and antigen-presenting molecules), ultimately rendering them more responsive to immunogenic stimuli within the TME. These findings support a model in which isoprenoid depletion, through modulation of small GTPases that regulate endosomal trafficking, enhances antigen uptake[160] and prolongs endosomal recycling, thereby increasing the surface expression of endosomal molecules such as MHC-II and CD40[113]. In parallel, defective prenylation activates the p38 MAPK pathway, promoting transcription of proinflammatory cytokine genes[110,151]. However, consistent with evidence that cytokine mRNAs can remain translationally silenced until stronger inflammatory signal occurs[161], these transcripts are unlikely to be translated in the absence of additional stimuli such as LPS. Nevertheless, their prior transcription enables a more rapid and robust cytokine response once such stimulation occurs.

Given the central role of isoprenoid depletion in mediating the immunomodulatory effects observed both in patients and in our preclinical models, future work should assess whether circulating or intracellular isoprenoid levels may serve as a biomarker to stratify responders versus non-responders to combined statin and anti-PD-1 therapy. Such metabolic readouts could provide a functional proxy for prenylation status and help identifying patients with greater susceptibility to statin-mediated immune activation.

This study has some limitations. First, the clinical component is retrospective, with inherent risks of selection bias, information/misclassification bias, and residual confounding. Although baseline variables were carefully curated, relevant covariates (e.g., co-medications, comorbidities, prior therapies, performance status) cannot be fully measured or adjusted for in a non-randomized setting; consequently, causal inference cannot be established, and the clinical associations should be considered hypothesis-generating. Second, the PBMC high-dimensional flow cytometry sub-analysis was constrained by the limited number of available samples and their random availability from two cohorts (n = 21), which reduces statistical power and increases susceptibility to imbalances in unmeasured covariates between statin users and non-users. In particular, differences in concomitant medications, likely heterogeneous across patients, may contribute to the observed immunophenotypes and could not be fully accounted for; residual confounding therefore cannot be excluded. Moreover, despite standardized staining, compensation, and analysis pipelines, batch effects and panel-specific technical variability cannot be entirely ruled out, and the multiple comparisons intrinsic to unsupervised clustering warrant cautious interpretation. Third, the preclinical findings underscore a time-dependence of statin effects: in the B16 model, starting simvastatin only after tumor implantation did not improve response to anti-PD-1, whereas pre-treatment was associated with delayed tumor growth and longer survival. This observation has implications for prospective trial design in immunotherapy-treated cancers: if statin-mediated immune modulation requires a lead-in period, initiating statin at the start of ICIs may be insufficient to yield a clinically meaningful effect. Future studies should be specifically addressed to elucidate the optimal exposure window defining the minimum duration of statin pre-treatment before ICI initiation. Finally, the generalizability of murine results is limited by the tumor model (B16), pharmacokinetic differences between species, and by the specific statin and ICI backbone employed; these factors may under- or over-estimate effects relative to human disease. Collectively, these limitations reinforce the exploratory nature of our observations and the need for prospective validation.

In conclusion, we demonstrate that patients diagnosed with melanoma receiving anti-PD1 immunotherapy and concomitant statin treatment for cardiovascular comorbidities exhibit improved clinical outcomes, including prolonged PFS and OS as well as higher

ORR. These clinical benefits are associated with an increased frequency of circulating APCs, particularly activated $CD11c^+$ monocytes, in PBMCs from responding patients. This observation was corroborated in preclinical melanoma models, which showed intratumoral accumulation of activated DCs and prolonged survival in mice treated with simvastatin in combination with anti-PD1 therapy. Mechanistically, we suggest that simvastatin promotes DC maturation by inhibiting isoprenoid biosynthesis and activating the p38 MAPK pathway, thereby shaping a TME more responsive to immune checkpoint blockade. Further studies are warranted to delineate the precise molecular mechanisms and to better define the APC subsets involved. Nonetheless, given their favorable safety profile and widespread clinical use of statins, our results provide a strong rationale for prospective trials in immunotherapy-treated cancers such as melanoma and NSCLC.

Chapter 6

BIBLIOGRAPHY

1. Tasdogan, A. *et al.* Cutaneous melanoma. *Nat Rev Dis Primers* 11, 23 (2025).

2. *Cancer Today: Melanoma of Skin - Age-Standardized Incidence Rate (World), Both Sexes*. https://gco.iarc.who.int/today (2022).

3. Associazione Italiana di Oncologia Medica (AIOM). *Line Guida AIOM 2023 - Melanoma*. (2023).

4. Long, G. V., Swetter, S. M., Menzies, A. M., Gershenwald, J. E. & Scolyer, R. A. Cutaneous melanoma. *The Lancet* 402, 485–502 (2023).

5. Cho, E., Rosner, B. A., Feskanich, D. & Colditz, G. A. Risk Factors and Individual Probabilities of Melanoma for Whites. *JCO* 23, 2669–2675 (2005).

6. Gandini, S. *et al.* Meta-analysis of risk factors for cutaneous melanoma: II. Sun exposure. *European Journal of Cancer* 41, 45–60 (2005).

7. Amaral, T. *et al.* Cutaneous melanoma: ESMO Clinical Practice Guideline for diagnosis, treatment and follow-up. *Annals of Oncology* 36, 10–30 (2025).

8. Gershenwald, J. E. *et al.* Melanoma staging: Evidence-based changes in the American Joint Committee on Cancer eighth edition cancer staging manual. *CA A Cancer J Clinicians* 67, 472–492 (2017).

9. Larkin, J. *et al.* Five-Year Survival with Combined Nivolumab and Ipilimumab in Advanced Melanoma. *N Engl J Med* 381, 1535–1546 (2019).

10. Donia, M. *et al.* The majority of patients with metastatic melanoma are not represented in pivotal phase III immunotherapy trials. *European Journal of Cancer* 74, 89–95 (2017).

11. Donia, M. *et al.* The real-world impact of modern treatments on the survival of patients with metastatic melanoma. *European Journal of Cancer* 108, 25–32 (2019).

12. Long, G. V. *et al.* Adjuvant Dabrafenib plus Trametinib in Stage III *BRAF* -Mutated Melanoma. *N Engl J Med* 377, 1813–1823 (2017).

13. Eggermont, A. M. M. *et al.* Adjuvant Pembrolizumab versus Placebo in Resected Stage III Melanoma. *N Engl J Med* 378, 1789–1801 (2018).

14. Luke, J. J. *et al.* Pembrolizumab versus placebo as adjuvant therapy in completely resected stage IIB or IIC melanoma (KEYNOTE-716): a randomised, double-blind, phase 3 trial. *The Lancet* 399, 1718–1729 (2022).

15. Long, G. V. *et al.* Prognostic and Clinicopathologic Associations of Oncogenic *BRAF* in Metastatic Melanoma. *JCO* 29, 1239–1246 (2011).

16. Robert, C. *et al.* Five-Year Outcomes with Dabrafenib plus Trametinib in Metastatic Melanoma. *N Engl J Med* 381, 626–636 (2019).

17. Dummer, R. *et al.* COLUMBUS 5-Year Update: A Randomized, Open-Label, Phase III Trial of Encorafenib Plus Binimetinib Versus Vemurafenib or Encorafenib in Patients With *BRAF* V600–Mutant Melanoma. *JCO* 40, 4178–4188 (2022).

18. Hodi, F. S. *et al.* Improved Survival with Ipilimumab in Patients with Metastatic Melanoma. *N Engl J Med* 363, 711–723 (2010).

19. Wolchok, J. D. *et al.* Final, 10-Year Outcomes with Nivolumab plus Ipilimumab in Advanced Melanoma. *N Engl J Med* 392, 11–22 (2025).

20. Robert, C. *et al.* Pembrolizumab versus ipilimumab in advanced melanoma (KEYNOTE-006): post-hoc 5-year results from an open-label, multicentre, randomised, controlled, phase 3 study. *The Lancet Oncology* 20, 1239–1251 (2019).

21. Tawbi, H. A. *et al.* Three-Year Overall Survival With Nivolumab Plus Relatlimab in Advanced Melanoma From RELATIVITY-047. *JCO* 43, 1546–1552 (2025).

22. Atkins, M. B. *et al.* Combination Dabrafenib and Trametinib Versus Combination Nivolumab and Ipilimumab for Patients With Advanced *BRAF* -Mutant Melanoma: The DREAMseq Trial—ECOG-ACRIN EA6134. *JCO* 41, 186–197 (2023).

23. Ascierto, P. A. *et al.* Sequential immunotherapy and targeted therapy for metastatic BRAF V600 mutated melanoma: 4-year survival and biomarkers evaluation from the phase II SECOMBIT trial. *Nat Commun* 15, 146 (2024).

24. Tawbi, H. A. *et al.* Combined Nivolumab and Ipilimumab in Melanoma Metastatic to the Brain. *N Engl J Med* 379, 722–730 (2018).

25. Long, G. V. *et al.* Ipilimumab plus nivolumab versus nivolumab alone in patients with melanoma brain metastases (ABC): 7-year follow-up of a multicentre, open-label, randomised, phase 2 study. *The Lancet Oncology* 26, 320–330 (2025).

26. Di Giacomo, A. M. *et al.* Primary Analysis and 4-Year Follow-Up of the Phase III NIBIT-M2 Trial in Melanoma Patients With Brain Metastases. *Clinical Cancer Research* 27, 4737–4745 (2021).

27. Galon, J. *et al.* Type, Density, and Location of Immune Cells Within Human Colorectal Tumors Predict Clinical Outcome. *Science* 313, 1960–1964 (2006).

28. Chen, D. S. & Mellman, I. Elements of cancer immunity and the cancer–immune set point. *Nature* 541, 321–330 (2017).

29. Bruni, D., Angell, H. K. & Galon, J. The immune contexture and Immunoscore in cancer prognosis and therapeutic efficacy. *Nat Rev Cancer* 20, 662–680 (2020).

30. Pagès, F. *et al.* International validation of the consensus Immunoscore for the classification of colon cancer: a prognostic and accuracy study. *The Lancet* 391, 2128–2139 (2018).

31. Gajewski, T. F., Schreiber, H. & Fu, Y.-X. Innate and adaptive immune cells in the tumor microenvironment. *Nat Immunol* 14, 1014–1022 (2013).

32. Galluzzi, L., Buqué, A., Kepp, O., Zitvogel, L. & Kroemer, G. Immunogenic cell death in cancer and infectious disease. *Nat Rev Immunol* 17, 97–111 (2017).

33. Kroemer, G., Galassi, C., Zitvogel, L. & Galluzzi, L. Immunogenic cell stress and death. *Nat Immunol* 23, 487–500 (2022).

34. Galluzzi, L., Buqué, A., Kepp, O., Zitvogel, L. & Kroemer, G. Immunological Effects of Conventional Chemotherapy and Targeted Anticancer Agents. *Cancer Cell* 28, 690–714 (2015).

35. Mole, R. H. Whole Body Irradiation—Radiobiology or Medicine? *The British Journal of Radiology* 26, 234–241 (1953).

36. Demaria, S. & Formenti, S. C. The abscopal effect 67 years later: from a side story to center stage. *The British Journal of Radiology* 93, 20200042 (2020).

37. Demaria, S., Coleman, C. N. & Formenti, S. C. Radiotherapy: Changing the Game in Immunotherapy. *Trends in Cancer* 2, 286–294 (2016).

38. Postow, M. A. *et al.* Immunologic Correlates of the Abscopal Effect in a Patient with Melanoma. *N Engl J Med* 366, 925–931 (2012).

39. Formenti, S. C. *et al.* Radiotherapy induces responses of lung cancer to CTLA-4 blockade. *Nat Med* 24, 1845–1851 (2018).

40. Kwilas, A. R. In the field: exploiting the untapped potential of immunogenic modulation by radiation in combination with immunotherapy for the treatment of cancer. *Front. Oncol.* 2, (2012).

41. Gasser, S., Orsulic, S., Brown, E. J. & Raulet, D. H. The DNA damage pathway regulates innate immune system ligands of the NKG2D receptor. *Nature* 436, 1186–1190 (2005).

42. Demaria, S. & Formenti, S. C. Sensors of ionizing radiation effects on the immunological microenvironment of cancer. *International Journal of Radiation Biology* 83, 819–825 (2007).

43. Antonia, S. J. *et al.* Durvalumab after Chemoradiotherapy in Stage III Non–Small-Cell Lung Cancer. *N Engl J Med* 377, 1919–1929 (2017).

44. Spigel, D. R. *et al.* Five-Year Survival Outcomes From the PACIFIC Trial: Durvalumab After Chemoradiotherapy in Stage III Non–Small-Cell Lung Cancer. *JCO* 40, 1301–1311 (2022).

45. Cheng, Y. *et al.* Durvalumab after Chemoradiotherapy in Limited-Stage Small-Cell Lung Cancer. *N Engl J Med* 391, 1313–1327 (2024).

46. Machiels, J.-P. *et al.* Pembrolizumab plus concurrent chemoradiotherapy versus placebo plus concurrent chemoradiotherapy in patients with locally advanced squamous cell carcinoma of the head and neck (KEYNOTE-412): a randomised, double-blind, phase 3 trial. *The Lancet Oncology* 25, 572–587 (2024).

47. Saddawi-Konefka, R. *et al.* The tumor-sentinel lymph node immuno-migratome reveals $CCR7^{+}$ dendritic cells drive response to sequenced immunoradiotherapy. *Nat Commun* 16, 6578 (2025).

48. Erinjeri, J. P. *et al.* Immunotherapy and the Interventional Oncologist: Challenges and Opportunities—A Society of Interventional Oncology White Paper. *Radiology* 292, 25–34 (2019).

49. Saldanha, E. F. *et al.* How we treat patients with metastatic uveal melanoma. *ESMO Open* 10, 104496 (2025).

50. National Comprehensive Cancer Network. *NCCN Guidelines Version 1.2025: Uveal Melanoma*. (2025).

51. Zager, J. S. *et al.* Efficacy and Safety of the Melphalan/Hepatic Delivery System in Patients with Unresectable Metastatic Uveal Melanoma: Results from an Open-Label, Single-Arm, Multicenter Phase 3 Study. *Ann Surg Oncol* 31, 5340–5351 (2024).

52. Minor, D. R. *et al.* A Pilot Study of Hepatic Irradiation with Yttrium-90 Microspheres Followed by Immunotherapy with Ipilimumab and Nivolumab for Metastatic Uveal Melanoma. *Cancer Biotherapy and Radiopharmaceuticals* 37, 11–16 (2022).

53. Tong, T. M. L. *et al.* Combining Melphalan Percutaneous Hepatic Perfusion with Ipilimumab Plus Nivolumab in Advanced Uveal Melanoma: First Safety and Efficacy Data from the Phase Ib Part of the Chopin Trial. *Cardiovasc Intervent Radiol* 46, 350–359 (2023).

54. De La Torre-Aláez, M. *et al.* Nivolumab after selective internal radiation therapy for the treatment of hepatocellular carcinoma: a phase 2, single-arm study. *J Immunother Cancer* 10, e005457 (2022).

55. Moore, A. E. Inhibition of growth of five transplantable mouse tumors by the virus of Russian far east encephalitis. *Cancer* 4, 375–382 (1951).

56. Smith, R. R., Huebner, R. J., Rowe, W. P., Schatten, W. E. & Thomas, L. B. Studies on the use of viruses in the treatment of carcinoma of the cervix. *Cancer* 9, 1211–1218 (1956).

57. Andtbacka, R. H. I. *et al.* Final analyses of OPTiM: a randomized phase III trial of talimogene laherparepvec versus granulocyte-macrophage colony-stimulating factor in unresectable stage III–IV melanoma. *j. immunotherapy cancer* 7, 145 (2019).

58. Chesney, J. A. *et al.* Talimogene laherparepvec in combination with ipilimumab versus ipilimumab alone for advanced melanoma: 5-year final analysis of a multicenter, randomized, open-label, phase II trial. *J Immunother Cancer* 11, e006270 (2023).

59. Kao, K.-C., Vilbois, S., Tsai, C.-H. & Ho, P.-C. Metabolic communication in the tumour–immune microenvironment. *Nat Cell Biol* 24, 1574–1583 (2022).

60. Warburg, O., Wind, F. & Negelein, E. THE METABOLISM OF TUMORS IN THE BODY. *Journal of General Physiology* 8, 519–530 (1927).

61. Vander Heiden, M. G., Cantley, L. C. & Thompson, C. B. Understanding the Warburg Effect: The Metabolic Requirements of Cell Proliferation. *Science* 324, 1029–1033 (2009).

62. Pavlova, N. N. & Thompson, C. B. The Emerging Hallmarks of Cancer Metabolism. *Cell Metabolism* 23, 27–47 (2016).

63. Nicklin, P. *et al.* Bidirectional Transport of Amino Acids Regulates mTOR and Autophagy. *Cell* 136, 521–534 (2009).

64. DeBerardinis, R. J. *et al.* Beyond aerobic glycolysis: Transformed cells can engage in glutamine metabolism that exceeds the requirement for protein and nucleotide synthesis. *Proc. Natl. Acad. Sci. U.S.A.* 104, 19345–19350 (2007).

65. Eagle, H. THE MINIMUM VITAMIN REQUIREMENTS OF THE L AND H E L A CELLS IN TISSUE CULTURE, THE PRODUCTION OF SPECIFIC VITAMIN DEFICIENCIES, AND THEIR CURE. *The Journal of Experimental Medicine* 102, 595–600 (1955).

66. Kusakabe, T. *et al.* Fatty Acid Synthase Is Expressed Mainly in Adult Hormone-sensitive Cells or Cells with High Lipid Metabolism and in Proliferating Fetal Cells[1]. *J Histochem Cytochem.* 48, 613–622 (2000).

67. Medes, G., Thomas, A. & Weinhouse, S. Metabolism of neoplastic tissue. IV. A study of lipid synthesis in neoplastic tissue slices in vitro. *Cancer Res* 13, 27–29 (1953).

68. Röhrig, F. & Schulze, A. The multifaceted roles of fatty acid synthesis in cancer. *Nat Rev Cancer* 16, 732–749 (2016).

69. Maier, T., Leibundgut, M. & Ban, N. The Crystal Structure of a Mammalian Fatty Acid Synthase. *Science* 321, 1315–1322 (2008).

70. Mullen, P. J., Yu, R., Longo, J., Archer, M. C. & Penn, L. Z. The interplay between cell signalling and the mevalonate pathway in cancer. *Nat Rev Cancer* 16, 718–731 (2016).

71. Ikonen, E. Cellular cholesterol trafficking and compartmentalization. *Nat Rev Mol Cell Biol* 9, 125–138 (2008).

72. Incardona, J. P. & Eaton, S. Cholesterol in signal transduction. *Current Opinion in Cell Biology* 12, 193–203 (2000).

73. Bensinger, S. J. *et al.* LXR Signaling Couples Sterol Metabolism to Proliferation in the Acquired Immune Response. *Cell* 134, 97–111 (2008).

74. Goldstein, J. L., DeBose-Boyd, R. A. & Brown, M. S. Protein Sensors for Membrane Sterols. *Cell* 124, 35–46 (2006).

75. Shimano, H. & Sato, R. SREBP-regulated lipid metabolism: convergent physiology — divergent pathophysiology. *Nat Rev Endocrinol* 13, 710–730 (2017).

76. Mullen, P. J., Yu, R., Longo, J., Archer, M. C. & Penn, L. Z. The interplay between cell signalling and the mevalonate pathway in cancer. *Nat Rev Cancer* 16, 718–731 (2016).

77. Ghosh, P. M. *et al.* Role of RhoA activation in the growth and morphology of a murine prostate tumor cell line. *Oncogene* 18, 4120–4130 (1999).

78. Saito, A. *et al.* Simvastatin inhibits growth via apoptosis and the induction of cell cycle arrest in human melanoma cells: *Melanoma Research* 18, 85–94 (2008).

79. Chojnacki, T. & Dallner, G. The biological role of dolichol. *Biochemical Journal* 251, 1–9 (1988).

80. Cheng, C. *et al.* Glucose-Mediated N-glycosylation of SCAP Is Essential for SREBP-1 Activation and Tumor Growth. *Cancer Cell* 28, 569–581 (2015).

81. Ernster, L. & Dallner, G. Biochemical, physiological and medical aspects of ubiquinone function. *Biochimica et Biophysica Acta (BBA) - Molecular Basis of Disease* 1271, 195–204 (1995).

82. Blank, C. U. *et al.* Defining 'T cell exhaustion'. *Nat Rev Immunol* 19, 665–674 (2019).

83. Chang, C.-H. *et al.* Posttranscriptional Control of T Cell Effector Function by Aerobic Glycolysis. *Cell* 153, 1239–1251 (2013).

84. Peng, M. *et al.* Aerobic glycolysis promotes T helper 1 cell differentiation through an epigenetic mechanism. *Science* 354, 481–484 (2016).

85. Ho, P.-C. *et al.* Phosphoenolpyruvate Is a Metabolic Checkpoint of Anti-tumor T Cell Responses. *Cell* 162, 1217–1228 (2015).

86. Rao, R. R., Li, Q., Odunsi, K. & Shrikant, P. A. The mTOR Kinase Determines Effector versus Memory CD8+ T Cell Fate by Regulating the Expression of Transcription Factors T-bet and Eomesodermin. *Immunity* 32, 67–78 (2010).

87. Sukumar, M. *et al.* Inhibiting glycolytic metabolism enhances CD8+ T cell memory and antitumor function. *J. Clin. Invest.* 123, 4479–4488 (2013).

88. Zhang, L. *et al.* Mammalian Target of Rapamycin Complex 2 Controls CD8 T Cell Memory Differentiation in a Foxo1-Dependent Manner. *Cell Reports* 14, 1206–1217 (2016).

89. Brand, A. *et al.* LDHA-Associated Lactic Acid Production Blunts Tumor Immunosurveillance by T and NK Cells. *Cell Metabolism* 24, 657–671 (2016).

90. Fernández-Ramos, A. A., Poindessous, V., Marchetti-Laurent, C., Pallet, N. & Loriot, M.-A. The effect of immunosuppressive molecules on T-cell metabolic reprogramming. *Biochimie* 127, 23–36 (2016).

91. Gropper, Y. *et al.* Culturing CTLs under Hypoxic Conditions Enhances Their Cytolysis and Improves Their Anti-tumor Function. *Cell Reports* 20, 2547–2555 (2017).

92. Ohta, A. *et al.* In vivo T Cell Activation in Lymphoid Tissues is Inhibited in the Oxygen-Poor Microenvironment. *Front. Immun.* 2, (2011).

93. Ugel, S., De Sanctis, F., Mandruzzato, S. & Bronte, V. Tumor-induced myeloid deviation: when myeloid-derived suppressor cells meet tumor-associated macrophages. *Journal of Clinical Investigation* 125, 3365–3376 (2015).

94. Munn, D. H. & Mellor, A. L. Indoleamine 2,3 dioxygenase and metabolic control of immune responses. *Trends in Immunology* 34, 137–143 (2013).

95. Mezrich, J. D. *et al.* An Interaction between Kynurenine and the Aryl Hydrocarbon Receptor Can Generate Regulatory T Cells. *The Journal of Immunology* 185, 3190–3198 (2010).

96. Sharma, M. D. *et al.* The PTEN pathway in T_{regs} is a critical driver of the suppressive tumor microenvironment. *Sci. Adv.* 1, e1500845 (2015).

97. Michalek, R. D. *et al.* Cutting Edge: Distinct Glycolytic and Lipid Oxidative Metabolic Programs Are Essential for Effector and Regulatory CD4+ T Cell Subsets. *The Journal of Immunology* 186, 3299–3303 (2011).

98. Hardie, D. G. AMP-activated/SNF1 protein kinases: conserved guardians of cellular energy. *Nat Rev Mol Cell Biol* 8, 774–785 (2007).

99. Everts, B. *et al.* Commitment to glycolysis sustains survival of NO-producing inflammatory dendritic cells. *Blood* 120, 1422–1431 (2012).

100. Gabrilovich, D. Mechanisms and functional significance of tumour-induced dendritic-cell defects. *Nat Rev Immunol* 4, 941–952 (2004).

101. Serafini, P., Borrello, I. & Bronte, V. Myeloid suppressor cells in cancer: Recruitment, phenotype, properties, and mechanisms of immune suppression. *Seminars in Cancer Biology* 16, 53–65 (2006).

102. Hossain, F. *et al.* Inhibition of Fatty Acid Oxidation Modulates Immunosuppressive Functions of Myeloid-Derived Suppressor Cells and Enhances Cancer Therapies. *Cancer Immunology Research* 3, 1236–1247 (2015).

103. Van Vlerken-Ysla, L., Tyurina, Y. Y., Kagan, V. E. & Gabrilovich, D. I. Functional states of myeloid cells in cancer. *Cancer Cell* 41, 490–504 (2023).

104. Kim, R. *et al.* Ferroptosis of tumour neutrophils causes immune suppression in cancer. *Nature* 612, 338–346 (2022).

105. Herber, D. L. *et al.* Lipid accumulation and dendritic cell dysfunction in cancer. *Nat Med* 16, 880–886 (2010).

106. Veglia, F. *et al.* Lipid bodies containing oxidatively truncated lipids block antigen cross-presentation by dendritic cells in cancer. *Nat Commun* 8, 2122 (2017).

107. Cao, W. *et al.* Oxidized Lipids Block Antigen Cross-Presentation by Dendritic Cells in Cancer. *The Journal of Immunology* 192, 2920–2931 (2014).

108. Su, P. *et al.* Enhanced Lipid Accumulation and Metabolism Are Required for the Differentiation and Activation of Tumor-Associated Macrophages. *Cancer Research* 80, 1438–1450 (2020).

109. Drenth, J. P. H. *et al.* Mutations in the gene encoding mevalonate kinase cause hyper-IgD and periodic fever syndrome. *Nat Genet* 22, 178–181 (1999).

110. Khan, O. M. *et al.* Geranylgeranyltransferase type I (GGTase-I) deficiency hyperactivates macrophages and induces erosive arthritis in mice. *J. Clin. Invest.* 121, 628–639 (2011).

111. Park, Y. H., Wood, G., Kastner, D. L. & Chae, J. J. Pyrin inflammasome activation and RhoA signaling in the autoinflammatory diseases FMF and HIDS. *Nat Immunol* 17, 914–921 (2016).

112. Akula, M. K. *et al.* Control of the innate immune response by the mevalonate pathway. *Nat Immunol* 17, 922–929 (2016).

113. Xia, Y. *et al.* The Mevalonate Pathway Is a Druggable Target for Vaccine Adjuvant Discovery. *Cell* 175, 1059-1073.e21 (2018).

114. Ma, X. *et al.* Cholesterol Induces CD8+ T Cell Exhaustion in the Tumor Microenvironment. *Cell Metabolism* 30, 143-156.e5 (2019).

115. Kidani, Y. *et al.* Sterol regulatory element–binding proteins are essential for the metabolic programming of effector T cells and adaptive immunity. *Nat Immunol* 14, 489–499 (2013).

116. Zhou, Q. D. *et al.* Interferon-mediated reprogramming of membrane cholesterol to evade bacterial toxins. *Nat Immunol* 21, 746–755 (2020).

117. Guo, C. *et al.* Cholesterol Homeostatic Regulator SCAP-SREBP2 Integrates NLRP3 Inflammasome Activation and Cholesterol Biosynthetic Signaling in Macrophages. *Immunity* 49, 842-856.e7 (2018).

118. Ito, A. *et al.* Cholesterol Accumulation in CD11c+ Immune Cells Is a Causal and Targetable Factor in Autoimmune Disease. *Immunity* 45, 1311–1326 (2016).

119. Westerterp, M. *et al.* Cholesterol Accumulation in Dendritic Cells Links the Inflammasome to Acquired Immunity. *Cell Metabolism* 25, 1294-1304.e6 (2017).

120. Nielsen, S. F., Nordestgaard, B. G. & Bojesen, S. E. Statin Use and Reduced Cancer-Related Mortality. *N Engl J Med* 367, 1792–1802 (2012).

121. Poynter, J. N. *et al.* Statins and the Risk of Colorectal Cancer. *N Engl J Med* 352, 2184–2192 (2005).

122. Cardwell, C. R., Hicks, B. M., Hughes, C. & Murray, L. J. Statin Use After Colorectal Cancer Diagnosis and Survival: A Population-Based Cohort Study. *JCO* 32, 3177–3183 (2014).

123. Ren, Q.-W. *et al.* Statin associated lower cancer risk and related mortality in patients with heart failure. *European Heart Journal* 42, 3049–3059 (2021).

124. Yu, O. *et al.* Use of Statins and the Risk of Death in Patients With Prostate Cancer. *JCO* 32, 5–11 (2014).

125. Scott, O. W., Tin Tin, S., Cavadino, A. & Elwood, J. M. Statin use and breast cancer-specific mortality and recurrence: a systematic review and meta-analysis including the role of immortal time bias and tumour characteristics. *Br J Cancer* 133, 539–554 (2025).

126. Bonovas, S., Filioussi, K., Flordellis, C. S. & Sitaras, N. M. Statins and the Risk of Colorectal Cancer: A Meta-Analysis of 18 Studies Involving More Than 1.5 Million Patients. *JCO* 25, 3462–3468 (2007).

127. Freedland, S. J. *et al.* Statin use and risk of prostate cancer and high-grade prostate cancer: results from the REDUCE study. *Prostate Cancer Prostatic Dis* 16, 254–259 (2013).

128. Shrank, W. H., Patrick, A. R. & Alan Brookhart, M. Healthy User and Related Biases in Observational Studies of Preventive Interventions: A Primer for Physicians. *J GEN INTERN MED* 26, 546–550 (2011).

129. Suissa, S. Immortal time bias in observational studies of drug effects. *Pharmacoepidemiology and Drug* 16, 241–249 (2007).

130. Dale, K. M., Coleman, C. I., Henyan, N. N., Kluger, J. & White, C. M. Statins and Cancer Risk: A Meta-analysis. *JAMA* 295, 74 (2006).

131. Newman, C. B. *et al.* Statin Safety and Associated Adverse Events: A Scientific Statement From the American Heart Association. *ATVB* 39, (2019).

132. Seckl, M. J. *et al.* Multicenter, Phase III, Randomized, Double-Blind, Placebo-Controlled Trial of Pravastatin Added to First-Line Standard Chemotherapy in Small-Cell Lung Cancer (LUNGSTAR). *JCO* 35, 1506–1514 (2017).

133. Jeong, I. G. *et al.* Adjuvant Low-dose Statin Use after Radical Prostatectomy: The PRO-STAT Randomized Clinical Trial. *Clinical Cancer Research* 27, 5004–5011 (2021).

134. Alarfi, H., Youssef, L. A. & Salamoon, M. A Prospective, Randomized, Placebo-Controlled Study of a Combination of Simvastatin and Chemotherapy in Metastatic Breast Cancer. *Journal of Oncology* 2020, 1–10 (2020).

135. Vos, W. G., Lutgens, E. & Seijkens, T. T. P. Statins and immune checkpoint inhibitors: a strategy to improve the efficacy of immunotherapy for cancer? *J Immunother Cancer* 10, e005611 (2022).

136. Liao, Y., Lin, Y., Ye, X. & Shen, J. Concomitant Statin Use and Survival in Patients With Cancer on Immune Checkpoint Inhibitors: A Meta-Analysis. *JCO Oncol Pract* 21, 989–1000 (2025).

137. Santoni, M. *et al.* Concomitant Use of Statins, Metformin, or Proton Pump Inhibitors in Patients with Advanced Renal Cell Carcinoma Treated with First-Line Combination Therapies. *Targ Oncol* 17, 571–581 (2022).

138. Cantini, L. *et al.* High-intensity statins are associated with improved clinical activity of PD-1 inhibitors in malignant pleural mesothelioma and advanced non-small cell lung cancer patients. *European Journal of Cancer* 144, 41–48 (2021).

139. Rossi, A. *et al.* Statins and immunotherapy: Togetherness makes strength The potential effect of statins on immunotherapy for NSCLC. *Cancer Reports* 4, e1368 (2021).

140. Cortellini, A. *et al.* Integrated analysis of concomitant medications and oncological outcomes from PD-1/PD-L1 checkpoint inhibitors in clinical practice. *J Immunother Cancer* 8, e001361 (2020).

141. Marrone, M. T. *et al.* Statin Use With Immune Checkpoint Inhibitors and Survival in Nonsmall Cell Lung Cancer. *Clinical Lung Cancer* 26, 201–209 (2025).

142. Dutertre, C.-A. *et al.* Single-Cell Analysis of Human Mononuclear Phagocytes Reveals Subset-Defining Markers and Identifies Circulating Inflammatory Dendritic Cells. *Immunity* 51, 573-589.e8 (2019).

143. Bourdely, P. *et al.* Transcriptional and Functional Analysis of CD1c+ Human Dendritic Cells Identifies a CD163+ Subset Priming CD8+CD103+ T Cells. *Immunity* 53, 335-352.e8 (2020).

144. Lazarus, J. *et al.* Mathematical Modeling of the Metastatic Colorectal Cancer Microenvironment Defines the Importance of Cytotoxic Lymphocyte Infiltration and Presence of PD-L1 on Antigen Presenting Cells. *Ann Surg Oncol* 26, 2821–2830 (2019).

145. Lugli, E., Galletti, G., Boi, S. K. & Youngblood, B. A. Stem, Effector, and Hybrid States of Memory CD8+ T Cells. *Trends in Immunology* 41, 17–28 (2020).

146. McLane, L. M., Abdel-Hakeem, M. S. & Wherry, E. J. CD8 T Cell Exhaustion During Chronic Viral Infection and Cancer. *Annu. Rev. Immunol.* 37, 457–495 (2019).

147. Ng Tang, D. *et al.* Increased Frequency of ICOS+ CD4 T Cells as a Pharmacodynamic Biomarker for Anti-CTLA-4 Therapy. *Cancer Immunology Research* 1, 229–234 (2013).

148. Georgiev, P. *et al.* Reverse Translating Molecular Determinants of Anti–Programmed Death 1 Immunotherapy Response in Mouse Syngeneic Tumor Models. *Molecular Cancer Therapeutics* 21, 427–439 (2022).

149. Bleve, A. *et al.* RORγ Bridges Cancer-Driven Lipid Dysmetabolism and Myeloid Immunosuppression. *Cancer Discovery* 15, 1505–1525 (2025).

150. Kuijk, L. M. *et al.* HMG-CoA reductase inhibition induces IL-1β release through Rac1/PI3K/PKB-dependent caspase-1 activation. *Blood* 112, 3563–3573 (2008).

151. Akula, M. K. *et al.* Protein prenylation restrains innate immunity by inhibiting Rac1 effector interactions. *Nat Commun* 10, 3975 (2019).

152. Dang, E. V. & Cyster, J. G. Loss of sterol metabolic homeostasis triggers inflammasomes — how and why. *Current Opinion in Immunology* 56, 1–9 (2019).

153. Ahern, T. P. *et al.* Statin Prescriptions and Breast Cancer Recurrence Risk: A Danish Nationwide Prospective Cohort Study. *JNCI Journal of the National Cancer Institute* 103, 1461–1468 (2011).

154. Villablanca, E. J. *et al.* Tumor-mediated liver X receptor-α activation inhibits CC chemokine receptor-7 expression on dendritic cells and dampens antitumor responses. *Nat Med* 16, 98–105 (2010).

155. Masters, S. L., Simon, A., Aksentijevich, I. & Kastner, D. L. *Horror Autoinflammaticus* : The Molecular Pathophysiology of Autoinflammatory Disease. *Annu. Rev. Immunol.* 27, 621–668 (2009).

156. Wu, H. *et al.* Functional Role of $CD11c^{+}$ Monocytes in Atherogenesis Associated With Hypercholesterolemia. *Circulation* 119, 2708–2717 (2009).

157. Philips, M. R. The perplexing case of the geranylgeranyl transferase-deficient mouse. *J Clin Invest* 121, 510–513 (2011).

158. Molnár, G., Dagher, M.-C., Geiszt, M., Settleman, J. & Ligeti, E. Role of Prenylation in the Interaction of Rho-Family Small GTPases with GTPase Activating Proteins. *Biochemistry* 40, 10542–10549 (2001).

159. Park, Y. H., Wood, G., Kastner, D. L. & Chae, J. J. Pyrin inflammasome activation and RhoA signaling in the autoinflammatory diseases FMF and HIDS. *Nat Immunol* 17, 914–921 (2016).

160. Benvenuti, F. *et al.* Requirement of Rac1 and Rac2 Expression by Mature Dendritic Cells for T Cell Priming. *Science* 305, 1150–1153 (2004).

161. Anderson, P. Post-transcriptional control of cytokine production. *Nat Immunol* 9, 353–359 (2008).